The role of waterfalls and knickzones in controlling the style and pace of landscape adjustment in the western San Gabriel Mountains, California

Roman A. DiBiase[1,†,§], Kelin X Whipple[2], Michael P. Lamb[1], and Arjun M. Heimsath[2]
[1]*Division of Geological and Planetary Sciences, California Institute of Technology, Pasadena, California 91125, USA*
[2]*School of Earth and Space Exploration, Arizona State University, Tempe, Arizona 85281, USA*

ABSTRACT

Bedrock rivers set the pace of landscape adjustment to tectonic and climatic forcing by transmitting signals of base-level change upstream through the channel network and ultimately to hillslopes. River incision is typically modeled as a monotonic function of bed shear stress or stream power, modulated by sediment tools and cover effects, but these models do not apply in channels with steep or vertical bedrock reaches due to changes in flow dynamics, hydraulic geometry, and bed cover. Here, we investigate how such knickzones (oversteepened channel reaches often containing waterfalls) influence the propagation of slope-break knickpoints that separate relict from adjusting topography, and thus the response times of landscapes to external forcing. We use a conceptual long-profile model to explore the consequences of waterfalls and knickzones on channel response and compare predictions to light detection and ranging (LiDAR) topography, field observations, and cosmogenic radionuclide data from Big Tujunga Creek, a 300 km^2 watershed in the San Gabriel Mountains, California. Three prominent knickzones along Big Tujunga Creek, characterized by numerous waterfalls, show contrasting behavior. For the upper knickzone, waterfalls align with bands of harder rock exposed on adjacent hillslopes, and between waterfalls, the channel is mantled by large (>2 m) boulders, indicating knickzone retreat is slow compared to predictions of slope-break knickpoint retreat from stream-power models, enhancing the preservation of an upstream relict landscape. The middle knickzone shows evidence for both fast and slow knickzone retreat, as well as significant deviations from predictions of uniform tributary knickpoint elevations derived from stream-power models. The lower knickzone is characterized by a waterfall and knickzone within an incised inner gorge that provide evidence of rapid retreat relative to background channel incision. Overall, we find a pattern of decreasing knickzone and waterfall retreat rate with distance upstream of the range front, beyond decreases predicted by simple area-dependent celerity models. Our results highlight that waterfalls and knickzones can both enhance and inhibit landscape adjustment, leading to divergent controls on the pace of landscape evolution.

INTRODUCTION

Changes in prevailing tectonic or climatic conditions can trigger periods of landscape adjustment that may last thousands to millions of years (e.g., Clark et al., 2005; Crosby and Whipple, 2006; Hilley and Arrowsmith, 2008; Wobus et al., 2010). Transient landscapes, where modern topography has yet to fully adjust to new boundary conditions, provide an opportunity to reconstruct the timing and magnitude of surface uplift over time scales that are difficult to obtain otherwise, and thus serve an important role in tectonic geomorphology (Schoenbohm et al., 2004; Clark et al., 2006; Whittaker et al., 2008; Kirby and Whipple, 2012; Miller et al., 2012). The erosional response to tectonic, climatic, and other (e.g., stream capture, wildfire, sea-level change) perturbations in upland landscapes has implications for interpreting sedimentary basin deposits (e.g., Paola et al., 1992; Blum and Tornqvist, 2000), determining the timing of orogenic decay (e.g., Baldwin et al., 2003), and assessing sedimentation hazards to life and property (e.g., Cannon and Gartner, 2005). Moreover, the study of transient landscapes informs models of landscape evolution by exposing complexities in surface process interactions that are not expressed during steady-state conditions (e.g., Whipple and Tucker, 2002). A key factor in these interpretations is a quantitative understanding of bedrock river incision processes; bedrock rivers set the relief structure of mountain ranges, and signals of base-level change are communicated upstream through the landscape by the channel network (e.g., Whipple et al., 2013).

Substantial efforts have been made in recent decades to identify and quantify the controls on long-term bedrock river incision (e.g., Howard et al., 1994; Whipple and Tucker, 1999; Sklar and Dietrich, 2004; Lamb et al., 2008a; Lague, 2014; Whipple et al., 2013). The most robust results have come from landscapes where assumptions of steady-state erosion and uniform rock uplift hold and predictions from a wide range of detachment-limited, transport-limited, and sediment-flux–dependent models converge (Whipple and Tucker, 2002; Tucker, 2004). In such landscapes, measured erosion rates generally track monotonically with metrics of stream power or bed shear stress, which are straightforward to extract from remotely sensed data (Ouimet et al., 2009; DiBiase et al., 2010; Bookhagen and Strecker, 2012). Following a change in base level, however, the style and timing of fluvial adjustment to new conditions are strongly model dependent (Whipple and Tucker, 2002; Gasparini et al., 2007) and sensitive to poorly constrained interactions among channel geometry, sediment flux, and changes in bed cover and roughness (e.g., Sklar and Dietrich, 2004; Finnegan et al., 2007; Johnson and Whipple, 2007; Valla et al., 2010; Cook et al., 2013). Spatial variations in the amount and caliber of sediment delivered to the channel network challenge assumptions built into stream-power incision laws (i.e., the use of drainage area as a proxy for sediment flux; Sklar and Dietrich, 2004; Lamb et al., 2008a), but these factors are difficult to quantify in the field. The complexities that emerge during transient or spatially nonuniform forcing are poorly constrained, but critical for quantitative reconstructions of landscape evolution.

†rdibiase@psu.edu.
§Present address: Department of Geosciences, Pennsylvania State University, University Park, Pennsylvania 16802, USA.

GSA Bulletin; March/April 2015; v. 127; no. 3/4; p. 539–559; doi: 10.1130/B31113.1; 13 figures; 2 tables; published online 22 October 2014.

In most detachment-limited river incision models, adjustment to new conditions is translated through the channel network as a wave of slope-break knickpoints (i.e., a stepwise change in channel steepness) that separate relict from adjusting landscapes (Whipple et al., 2013). However, the observed transient response of fluvial networks is rarely so straightforward and is often accompanied by the presence of oversteepened reaches or "knickzones" that may include one or more waterfalls (e.g., Crosby and Whipple, 2006; Hayakawa and Oguchi, 2006). These steep reaches are often characterized by changes in bed cover, channel geometry, and erosion process that are difficult to incorporate within a stream-power framework (Crosby and Whipple, 2006). Furthermore, assumptions of steady, uniform flow and low water-surface slopes common to most river incision models do not apply in steep or vertical reaches (Haviv et al., 2006; Lamb et al., 2007). Two questions emerge: Do knickzones and waterfalls influence the retreat rates of slope-break knickpoints, and thus landscape response times, in a manner that deviates from stream-power predictions? If so, what are the controls on river incision and waterfall retreat in these knickzones, and how do they influence landscape response time and slope-break knickpoint propagation?

Overall, it is unclear whether steep knickzones (including waterfalls) accelerate or slow fluvial response to changing base level. Typically, the influence of waterfalls on communicating signals of base-level change in active orogens is considered incidental to bedrock river incision processes (e.g., Kirby and Whipple, 2012). While workers have focused efforts on quantifying the retreat rates of waterfalls in natural (e.g., Seidl et al., 1997; Hayakawa and Matsukura, 2003; Crosby and Whipple, 2006; Haviv et al., 2006; Jansen et al., 2011; Lamb et al., 2014; Mackey et al., 2014) and experimental (e.g., Gardner, 1983; Frankel et al., 2007; Lamb and Dietrich, 2009) settings, the influence of waterfalls on fluvial long-profile evolution (and thus relief) remains largely unexplored, despite the fact that waterfalls can make up significant fractions of bedrock channel relief (e.g., Ortega et al., 2013). The only landscape evolution models that generate waterfalls in the absence of sudden base-level drop rely on negative feedbacks between slope and erosion rate present in bed load–abrasion river incision models (e.g., Sklar and Dietrich, 2004; Chatanantavet and Parker, 2009). Such models are invoked to explain patterns of fluvial hanging valleys (Wobus et al., 2006a; Crosby et al., 2007) and the persistence of steep topography in ancient orogens (Egholm et al., 2013), but they cannot account for migrating waterfalls and may not form altogether if erosion by suspended sediment is incorporated (Scheingross et al., 2014).

In this contribution, we explore how waterfalls and knickzones may either slow or accelerate landscape adjustment to base-level fall, using a conceptual river long-profile evolution model. We apply these predictions to Big Tujunga Creek, a 300 km^2 catchment in the western San Gabriel Mountains, California, which we interpret to be responding to a two-staged increase in rock uplift rate. Using a combination of light detection and ranging (LiDAR) digital elevation model (DEM) analysis, detailed field surveys, and new and published cosmogenic radionuclide data, we test whether knickzones and waterfalls in this landscape are "slow" or "fast" relative to expectations from stream-power–based erosion models that explain the behavior of steady-state channels. Last, we discuss the influence of waterfalls and knickzones on the spatial patterns of slope-break knickpoint retreat, and implications for preserving relict topography and extracting the history of climate and tectonics from transient landscapes.

CONCEPTUAL FRAMEWORK

We use a conceptual river long-profile evolution model to compare the geometric consequences of oversteepened knickzones and waterfalls on landscape response time scales. We present three examples of a bedrock river long-profile responding to a threefold sustained increase in relative base-level fall at its outlet: a detachment-limited case with no knickzones or waterfalls, and cases with an imposed knickzone or waterfall downstream of the slope-break knickpoint that retreats either fast or slow relative to the horizontal retreat rate of the slope-break knickpoint in the case with no knickzone. We focus on the case of a sustained increase in base-level fall because this is hypothesized to be the driving mechanism of relief generation in active orogens (e.g., Kirby and Whipple, 2012), as well as the mode of base-level fall in Big Tujunga Creek (Wobus et al., 2006a).

River Long-Profile Evolution: Stream Power, No Waterfalls

As a baseline case, consider a channel responding to a threefold increase in uplift rate following a detachment-limited stream-power incision law according to:

$$E \propto A^m S^n, \quad (1)$$

where E is erosion rate, A is upstream drainage area, S is channel slope, and m and n are exponents that depend on incision process (e.g., Seidl and Dietrich, 1992; Whipple and Tucker, 1999). Figure 1A shows the simple case of $m = 0.5$ and $n = 1$ (hereafter referred to as linear stream power) for a generic long profile for which the drainage area grows with distance downstream x following Hack's law ($A = x^{1.7}$; Whipple and Tucker, 1999). A key prediction common to most detachment-limited bedrock incision models is that changes in base level propagate upstream through the channel network as migrating slope-break knickpoints that separate relict from adjusted portions of the landscape (Fig. 1A; Howard et al., 1994; Seidl et al., 1994; Kirby and Whipple, 2012; Whipple et al., 2013). Differences between the upstream, relict channel and the downstream, adjusted reach can be quantified using the channel steepness index k_s, defined by:

$$k_s = SA^{\theta}, \quad (2)$$

where θ is a concavity index that typically ranges from 0.4 to 0.6 (Wobus et al., 2006b). When analyzing natural landscapes, it is convenient to recast Equation 2 in terms of a fixed reference concavity index θ_{ref} (Wobus et al., 2006b). The resulting normalized channel steepness index ($k_{sn} = SA^{\theta ref}$) can be thought of as a proxy for stream power, as well as a scale-independent metric of fluvial catchment relief (DiBiase et al., 2010). For the case of the stream-power incision model, θ is defined by the ratio m/n at steady state for the case of uniform uplift and erodibility. However, the scaling relationship of channel slope and drainage area following Flint's law ($S = k_s A^{-\theta}$; Flint, 1974) is general, independent of any specific river incision rule, and is readily incorporated into many models of bedrock river incision (Whipple et al., 2013).

Based solely on geometrical arguments, the horizontal retreat rate of a slope-break knickpoint V_{kp} is defined by:

$$V_{kp} = \frac{E_{ds} - E_{us}}{S_{ds} - S_{us}}, \quad (3)$$

where the subscripts "us" and "ds" correspond to values for channel reaches upstream and downstream of the slope-break, respectively (Finnegan, 2013). Thus, for typical slopes in mountain rivers, V_{kp} can be 10–100 times greater than local vertical incision rates. For the case of stream power, it can also be shown that when m and n do not vary, V_{kp} increases with $A^{m/n}$ following a sustained increase in base-level fall, resulting in a constant vertical migration rate and the implication that slope-break knickpoints on tributaries responding to a common base-level signal lie at the same elevation, assuming uniform relict and adjusting k_{sn} values within

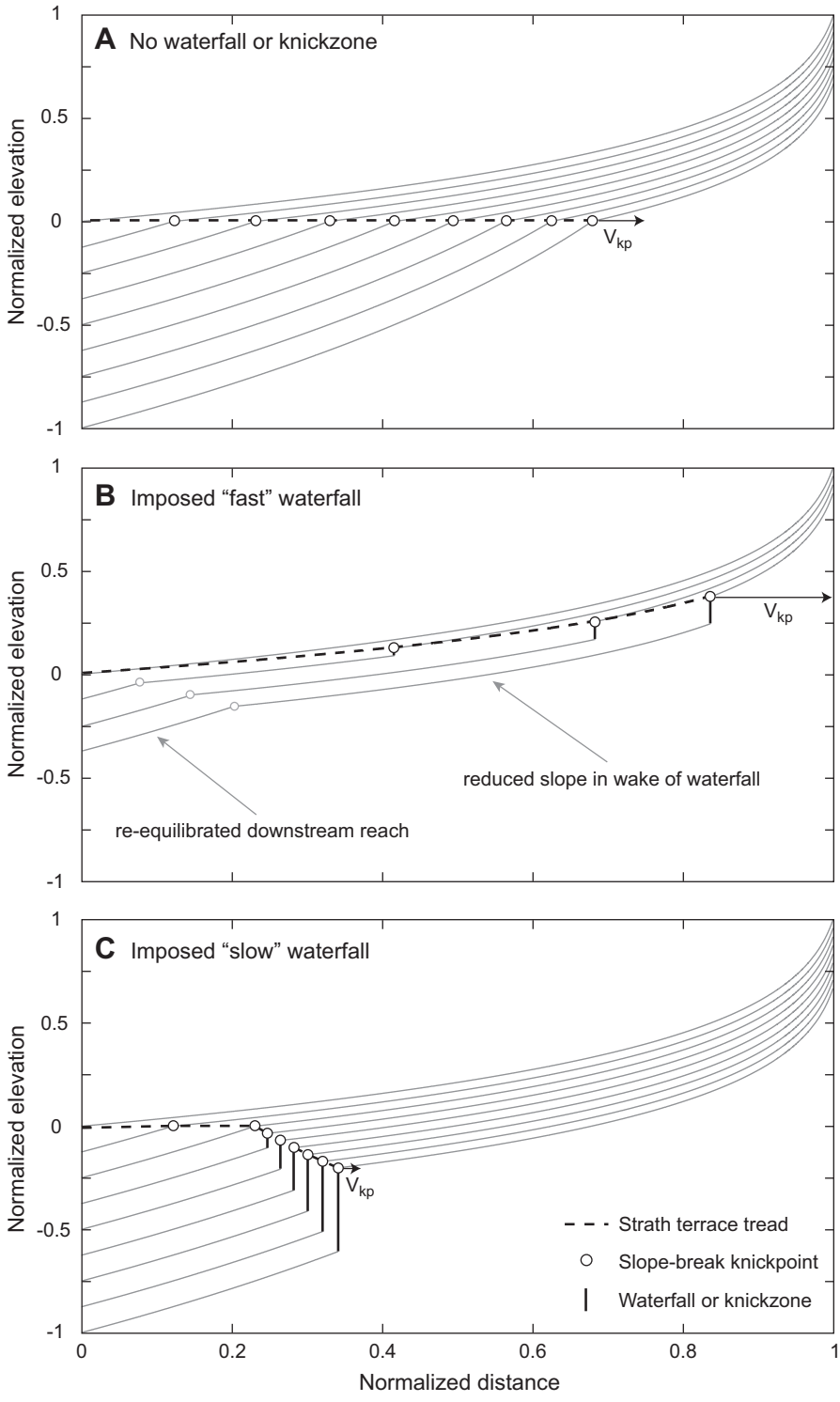

Figure 1. Conceptual channel long-profile evolution following a threefold increase in uplift rate for (A) linear stream power with no waterfalls (slope-break knickpoint only), (B) imposed "fast" waterfall or knickzone relative to the linear stream-power case (note that only the first four time steps are shown), and (C) imposed "slow" waterfall or knickzone beginning at the third time step. In all cases, frame of reference is fixed with respect to the initial profile through time. Black arrows indicate the relative magnitude of horizontal slope-break knickpoint or knickzone retreat rate V_{kp}, which determines the time scale of landscape adjustment to changing base level. For part B, the reduced slope channel reach in the wake of the fast waterfall or knickzone must eventually steepen to re-equilibrate with the new, higher uplift rate.

the catchment (Niemann et al., 2001; Wobus et al., 2006a). Furthermore, in the case of linear stream power, as the slope-break knickpoint retreats, it leaves behind a horizontal tread of strath terraces (Fig. 1A; Finnegan, 2013). Incision models that deviate from linear stream power can influence both the style and timing of profile evolution (e.g., Seidl et al., 1994; Whipple and Tucker, 2002; Attal et al., 2011; Royden and Perron, 2013), but the general behavior of a migrating slope-break knickpoint separating reaches of different channel steepness is common to most detachment-limited variants, and distinctive from the more diffusive response of transport-limited systems (Whipple and Tucker, 2002; Kirby and Whipple, 2012).

Influence of Knickzones on River Long-Profile Evolution

The transient adjustment of river long profiles is often marked by the presence of knickzones (locally steep channel reaches) that accompany slope-break knickpoints separating relict from adjusted portions of the landscape (e.g., Crosby and Whipple, 2006; Berlin and Anderson, 2007). In addition to heightened slopes, knickzones are often characterized by changes in bed cover, grain size, and channel geometry, which influence both the distribution of bed stresses as well as thresholds for erosion (Lague, 2014). In extreme cases, knickzones characterized by waterfalls indicate a switch in bedrock erosion process—the processes that govern waterfall retreat, such as plunge-pool drilling (Howard et al., 1994; Lamb et al., 2007), toppling (Lamb and Dietrich, 2009), and undercutting and mass wasting (Gilbert, 1907; Haviv et al., 2010), differ from those active along channel reaches with lower slopes (e.g., abrasion, plucking). As a result, it is plausible that changes in bed condition and incision process across knickzones may either limit or enhance the retreat rate of slope-break knickpoints.

We explored the geometrical consequences of introducing a knickzone or waterfall below the slope-break knickpoint using two end-member cases, depending on whether the knickzone retreats faster or slower than the horizontal migration of the slope-break knickpoint in the linear stream-power case. Because the mechanisms of waterfall and knickzone growth and retreat are poorly constrained, we simply imposed a vertical step that grows in time for illustrative purposes. However, we focus on general behavior that is common to all cases where the net influence of waterfalls or knickzones is to accelerate or delay landscape response relative to the baseline linear stream-power case (Fig. 1A).

If a knickzone forms and migrates rapidly by parallel slope retreat (Fig. 1B), there are two key geometrical consequences. First, the projected slope of time-transgressive strath terrace treads downstream of the knickzone will approach the modern stream gradient if retreat rates are fast relative to vertical incision upstream and downstream of the knickzone (e.g., Haviv et al., 2006; Finnegan, 2013). Second, the reach downstream of the waterfall or knickzone must be less steep than its final steady-state slope. Depending on the degree of this slope decrease, a wake of alluviation may develop as a result of imbalances between local transport capacity and upstream sediment supply. This decrease in slope occurs because rapid erosion due to knickpoint retreat locally and temporarily outpaces rock uplift. However, these downstream reaches must steepen eventually in order for the river to attain steady state between erosion and the new, higher uplift rate. Thus, the overall landscape response time may approach that of the linear stream-power case.

If a knickzone forms and retreats slowly (Fig. 1C), then it is possible for the downstream channel reach to be as steep or steeper than the linear stream-power case (Fig. 1A), depending on the details involving if and how the knickzone grows and retreats. In the extreme case of negligible waterfall or knickzone retreat, the downstream reach will continue to steepen as a hanging valley and will not reach steady state (Wobus et al., 2006a; Crosby et al., 2007). In contrast to the fast waterfall or knickzone case, the tread of strath terrace remnants will increase in elevation downstream, and as a result will be less likely to be preserved.

Although the knickzones imposed in Figures 1B and 1C have opposite effects on fluvial landscape response times and the nature of sediment delivery to basins, it is not possible to use a single long-profile to distinguish these two cases. This is because we do not know a priori the final steady-state steepness of the lower reach, and thus cannot evaluate the degree to which downstream channel slopes have been modified (e.g., Fig. 1B), or whether they are at a steady-state steepness following the long-term balance between uplift and incision. Additional information is needed to determine the relative retreat rates of knickzones, such as the patterns of preserved strath terraces (e.g., Finnegan, 2013) and tributary long profiles, measurements of incision rates, or evidence of local hillslope adjustment (Gallen et al., 2011; Mackey et al., 2014). Without these constraints, interpretations of base-level history based on river long-profile analysis using stream-power models may either underestimate landscape response times if knickzones are slow or stalled, or overestimate landscape response times if knickzones are fast.

FIELD SETTING

To further investigate the role of knickzones and waterfalls on fluvial long profiles, we analyzed the channel network of Big Tujunga Creek and its tributaries in the western San Gabriel Mountains, California. Big Tujunga Creek has been used as a type example of a channel network responding to a sustained increase in uplift rate, and it has been argued to match predictions from detachment-limited stream-power models similar to the example in Figure 1A (Wobus et al., 2006a, 2006b; Perron and Royden, 2013). Despite the general correspondence with expectation (i.e., the presence of discrete slope-break knickpoints on tributary and main-stem channels), close inspection reveals numerous deviations from the patterns predicted by simple stream-power models that may hold important clues about the richer behavior of natural systems. First, we find that slope-break knickpoints on main-stem and major tributary channels do not lie on an elevation contour as predicted. Second, we find that Big Tujunga Creek and its tributaries are characterized by numerous waterfalls, inner gorges, and strath terraces that are at odds with predictions from stream-power–based models of bedrock river incision, and that require consideration of the potential role of knickzones and waterfalls in influencing landscape response times. In this section, we outline the geologic and geomorphic framework for Big Tujunga Creek and the San Gabriel Mountains and provide an overview of the regional topography and published erosion rate data.

Overview of the San Gabriel Mountains

The San Gabriel Mountains lie in the central Transverse Ranges of southern California (Fig. 2), bounded by the right-lateral San Andreas fault to the north, and a series of north-dipping thrust faults (Sierra Madre fault zone, Cucamonga fault zone) to the south, which accommodate contraction necessitated by a large restraining bend in the San Andreas fault. The current fault configuration responsible for active uplift of the San Gabriel Mountains is thought to have initiated ca. 5–7 Ma, when dextral slip on the San Gabriel fault transferred to the current trace of the San Andreas fault (Matti and Morton, 1993). In the core of the San Gabriel Mountains, topographic relief, decadal sediment flux (Lavé and Burbank, 2004; Lamb et al., 2011), millennial erosion rates (DiBiase et al., 2010; Heimsath et al., 2012), and long-term (million-year time scale) exhumation rates (Spotila et al., 2002) generally increase from west to east. The surprising agreement between measures of erosion spanning decadal, millennial, and million-year time scales, which also broadly match Holocene slip rate estimates for the Sierra Madre fault zone and Cucamonga fault zone (Peterson and Wesnousky, 1994; Lindvall and Rubin, 2008), suggests that the position of the San Gabriel Mountains along the San Andreas fault has sustained an east-west gradient in rock uplift for at least the past 5 m.y. Palinspastic reconstructions of the transverse ranges by Blythe et al. (2002) constrained by apatite fission-track and (U-Th)/He thermochronology support this interpretation.

In contrast to the strong east-west gradient in rock uplift, climate and rock strength do not vary systematically across the San Gabriel Mountains. Although mean annual precipitation (MAP) varies with elevation—the highest elevations receive in excess of 1 m/yr, and the northern flank of the San Gabriel Mountains lies in a rain shadow with MAP as low as 0.2 m/yr—the majority of the San Gabriel Mountains receives ~0.6–1.0 m/yr of precipitation (PRISM, www.prism.oregonstate.edu). Runoff is even more uniform, and historical streamflow records from throughout the San Gabriel Mountains indicate that discharge parameters are similar across the range with respect to mean daily runoff, decadal maximum runoff, and flood variability (Lavé and Burbank, 2004; DiBiase and Whipple, 2011). Mean daily runoff varies by only 30% across catchments spanning two orders of magnitude in drainage area, and the distributions of normalized mean daily runoff for these catchments exhibit similar power-law tails for large events (DiBiase and Whipple, 2011). Variations in rock strength are more difficult to quantify, but in general, the San Gabriel Mountains consist of highly fractured Precambrian and Mesozoic crystalline rock. Extensive decimeter-scale weaknesses tend to minimize differences in rock mass strength among lithologies, and while exposed rock is common across the San Gabriel Mountains, outcrops tend to be blocky (fractured at the decimeter to meter scale) rather than massive (DiBiase et al., 2012). Furthermore, catchments with similar relief and climate draining schist, granodiorite, gneiss, and anorthosite exhibit similar erosion rates, suggesting a minimal variation in rock strength among lithologies at the landscape scale (DiBiase et al., 2010), although smaller-scale heterogeneities in erosional resistance may play a role in modulating the location and retreat rate of individual waterfalls.

DiBiase et al. (2010) exploited this spatial variation in rock uplift rate to quantify the topographic controls on erosion rate in a landscape with minimal variation of climate and rock strength. Focusing on catchments interpreted to be at or near topographic steady state (i.e., no

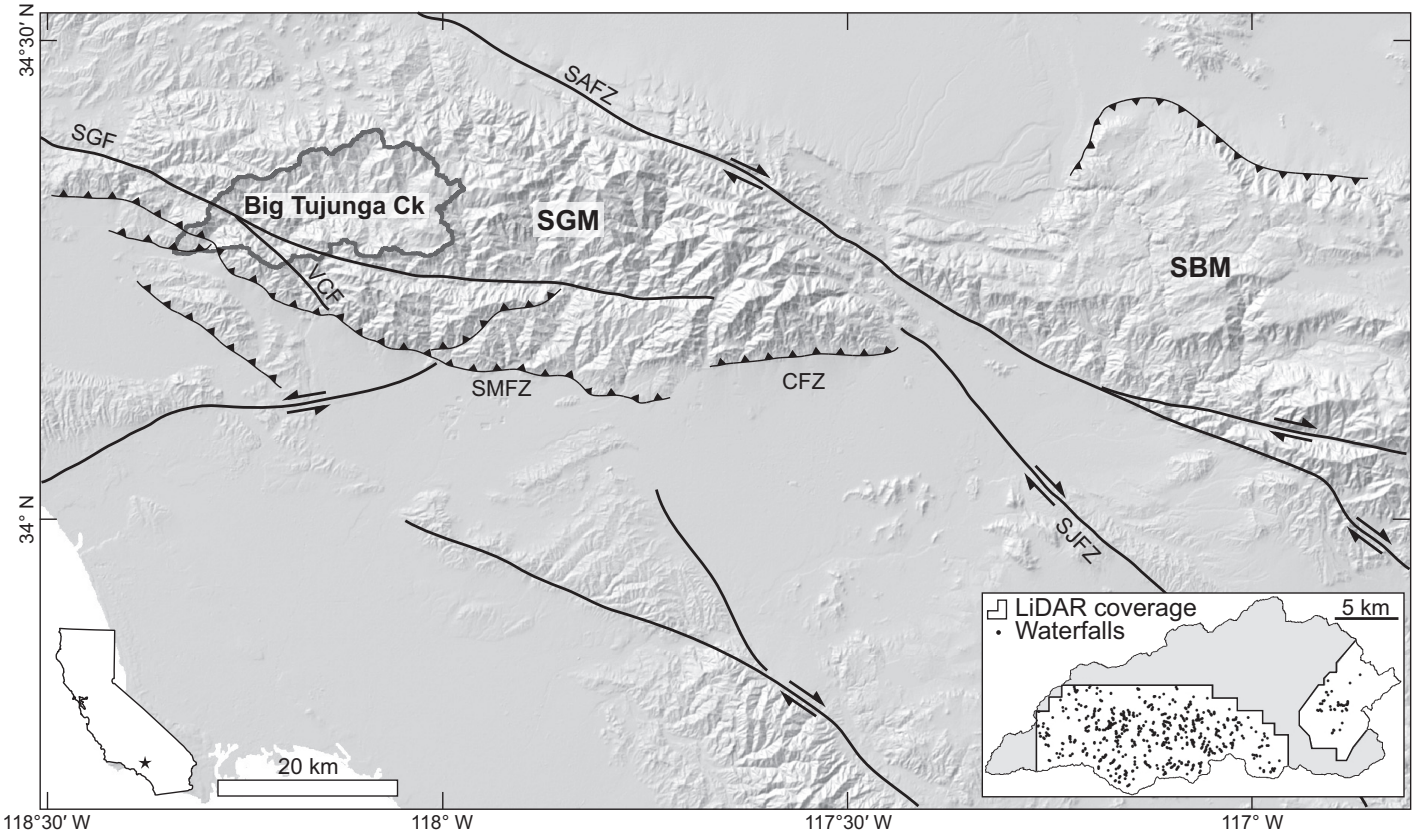

Figure 2. Shaded relief map of San Gabriel Mountains (SGM), showing location in southern California relative to major fault systems (SAFZ—San Andreas fault zone; SJFZ—San Jacinto fault zone; SGF—San Gabriel fault; SMFZ—Sierra Madre fault zone; VCF—Vasquez Creek Fault) and San Bernardino Mountains (SBM). Thick outline highlights drainage basin of Big Tujunga Creek and extent of Figure 4. Inset shows spatial extent of 1 m light detection and ranging (LiDAR) data, and the distribution of >800 mapped waterfalls along Big Tujunga Creek and its tributaries.

major slope-break knickpoints in channels and similar hillslope properties throughout watershed), DiBiase et al. (2010) compared mean hillslope angle and channel steepness index to catchment-averaged erosion rates determined from cosmogenic ^{10}Be concentrations in stream sands, which range from 30 to 1100 m/m.y. They showed that while mean hillslope angle reaches a threshold value at ~300 m/m.y., the normalized channel steepness index k_{sn} of streams within each catchment increases monotonically with erosion rate E across the San Gabriel Mountains. The pattern of higher uplift rates corresponding to higher channel steepness index and erosion rate, but similar concavity index ($\theta = 0.45$), is broadly consistent with predictions of a wide range of steady-state stream-power–based models (DiBiase et al., 2010). Combining this erosion rate data set with hydrologic records and field observations of channel width, grain size, and sediment cover, DiBiase and Whipple (2011) showed that the nonlinear relationship between k_{sn} and E for channels at or close to steady state can be simply explained by a linear stream-power model that incorporates a full distribution of floods and a threshold to erosion (e.g., Tucker, 2004; Lague et al., 2005). Additionally, DiBiase and Whipple (2011) showed that steady-state channels in the San Gabriel Mountains are characterized by a thin, mostly continuous sediment cover, where channel width can be approximated by a power-law dependence on drainage area that is independent of slope. Thus, for steady-state channels, spatial variations in slope and drainage area appear to sufficiently capture the key processes responsible for long-term bedrock river incision. These observations form the baseline for our comparison of channel behavior across knickpoints, which as we describe herein contrasts dramatically with observations of steady-state San Gabriel Mountains channels.

Big Tujunga Creek

Big Tujunga Creek is the largest ($A = 300$ km^2) of a series of drainages along the western front range of the San Gabriel Mountains that are characterized by numerous waterfalls along their tributary and main-stem channels (Fig. 2, inset), in contrast to observations from graded channels that lack slope-break knickpoints (DiBiase and Whipple, 2011). An examination of hillslope morphology and river long-profiles highlights three distinct physiographic zones within the catchment of Big Tujunga Creek, which are separated by prominent slope-break knickpoints in the stream network (Fig. 3) and more diffuse slope transitions along hillsides (Fig. 4).

The uppermost zone (PZ1: 1550–2500 m elevation) is characterized by a low-relief landscape with a mean hillslope angle of 15° and a mean k_{sn} of 20 m$^{0.9}$. Road cuts and the prevalence of tors up to 10 m in height indicate a deeply weathered corestone topography that is similar in character to surfaces identified in the Mojave Desert and the Big Bear Plateau in the San Bernardino Mountains (Spotila et al., 2002). Cosmogenic ^{10}Be-derived catchment-averaged erosion rates (DiBiase et al., 2010) and soil production rates (Heimsath et al., 2012)

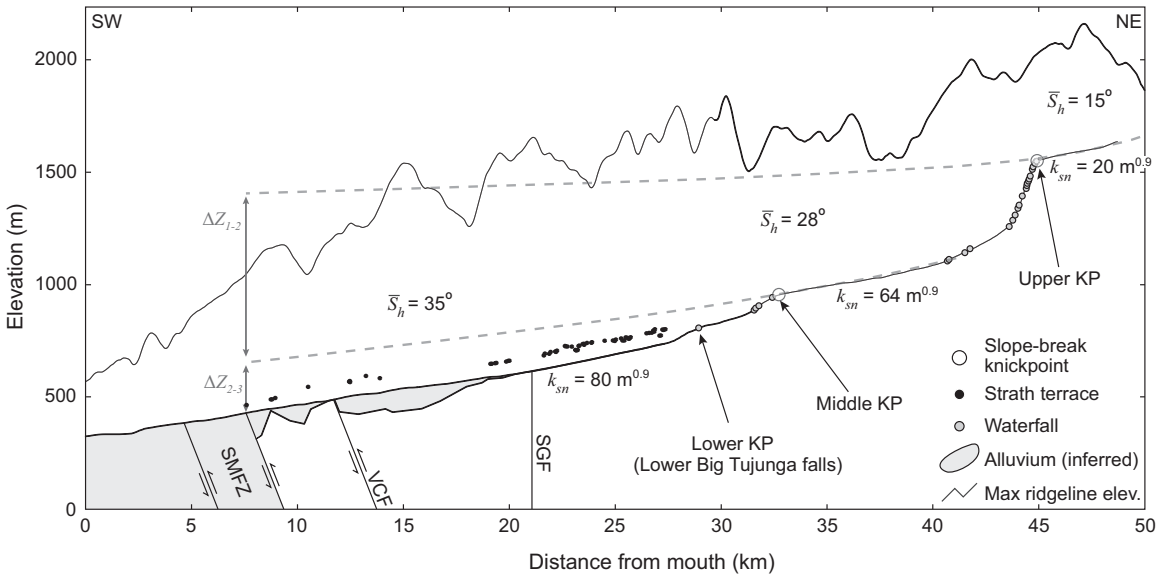

Figure 3. Cross section of Big Tujunga Creek, showing the main-stem channel long profile and the maximum ridgeline elevation along a 10-km-wide swath parallel to the main stem. Mean hillslope angle (S_h) and normalized channel steepness index (k_{sn}) for the three physiographic zones are indicated, along with the locations of the three prominent main-stem knickpoints (KP). Dashed lines indicate relict channel long-profile projections used for reconstructing surface uplift history (see text for description). Fault abbreviations are same as in Figure 2. We estimated the depth to bedrock by assuming a trapezoidal bedrock cross section with side slopes of 45° and a basal width of 70 m and converted valley width to sediment depth accordingly.

indicate a landscape-averaged erosion rate for PZ1 of 45 ± 5 m/m.y.

The intermediate physiographic zone (PZ2: 1000–1550 m) is characterized by a mean hillslope angle of 28° and a mean k_{sn} of 64 m$^{0.9}$. Hillslopes here are predominantly soil mantled, but the underlying bedrock is less weathered than PZ1, and soils tend to be thinner (Dixon et al., 2012; Heimsath et al., 2012). Soil production rates and catchment-averaged erosion rates determined for tributary basins entirely within PZ2 indicate a landscape-averaged erosion rate of 165 ± 30 m/m.y. (DiBiase et al., 2010; Heimsath et al., 2012; Mueller, 2013).

The lowermost physiographic zone (PZ3: <1000 m) is defined by the gorge of lower Big Tujunga Creek and its tributaries. Hillslopes tend to be steep (>35°) and rocky (DiBiase et al., 2012), and tributary channels are characterized by numerous bedrock steps and waterfalls. Determining the erosion rate for PZ3 is challenging due to a lack of fully adjusted channels—most tributary catchments span PZ2 and PZ3, and thus detrital ^{10}Be measurements record some combination of erosion rates from PZ2, PZ3, and any transient contribution from waterfall and inner gorge faces (e.g., Reinhardt et al., 2007; Mackey et al., 2014). Taken at face value, measurements from Lucas Creek, Clear Creek, and Trail Creek indicate modern erosion rates of 0.3–0.4 mm/yr for catchments spanning PZ2 and PZ3 (DiBiase et al., 2010). Additionally, erosion rates from smaller catchments along the range front adjacent to Big Tujunga Creek range from 0.5 to 1.0 mm/yr (DiBiase et al., 2012) and are in general agreement with estimates of Holocene vertical slip rates along the Sierra Madre fault zone (Lindvall and Rubin, 2008). Thus, we estimate the mean erosion rate of PZ3 to be 500 ± 200 m/m.y. A third knickzone along the main stem of Big Tujunga Creek, headed by Lower Big Tujunga Falls (785 m elevation), delineates an inner gorge within PZ3. Herein, we treat this lower knickzone as a separate base-level signal, but we do not define a fourth physiographic zone due to its limited areal extent and similar topographic characteristics to PZ3.

Tectonic History Encoded by River Long Profiles

The three physiographic zones in Big Tujunga Creek are characterized by distinct topographic characteristics and span nearly an order of magnitude in erosion rate. The physiographic zones and associated slope-break knickpoints do not match up with lithologic or tectonic boundaries but are instead consistent with upstream-propagating waves of incision (Wobus et al., 2006a; Perron and Royden, 2013; Whipple et al., 2013). Furthermore, the progressive steepening of the landscape that is associated with an increase in measured erosion rates is consistent with a stepwise increase in base-level fall associated with increased slip rates along the southern range-bounding thrust faults.

The history of surface uplift encoded by Big Tujunga Creek can be analyzed using projected river long profiles as dynamic geomorphic markers, with constraints on timing provided by estimates of uplift and erosion rates (e.g., Schoenbohm et al., 2004; Clark et al., 2005; Kirby and Whipple, 2012). The time since the most recent increase in base-level fall (ΔT_2, age of the lower knickpoint) can be calculated as:

$$\Delta T_2 = \frac{\Delta Z_{2-3}}{(E_3 - E_2)}, \quad (4)$$

where ΔZ_{2-3} is the difference in elevation between the current base level and the projected profile of the intermediate reach, and E_3 and E_2 are the erosion rates (averaged over ΔT_2) of the lowermost and intermediate channel segments, respectively (PZ3 and PZ2). The time since the prior increase in base-level fall (ΔT_1, age of the upper knickpoint) can be determined similarly:

$$\Delta T_1 = \Delta T_2 + \frac{\Delta Z_{1-2}}{(E_2 - E_1)}, \quad (5)$$

where ΔZ_{1-2} is the difference in elevation between the upper and intermediate projected

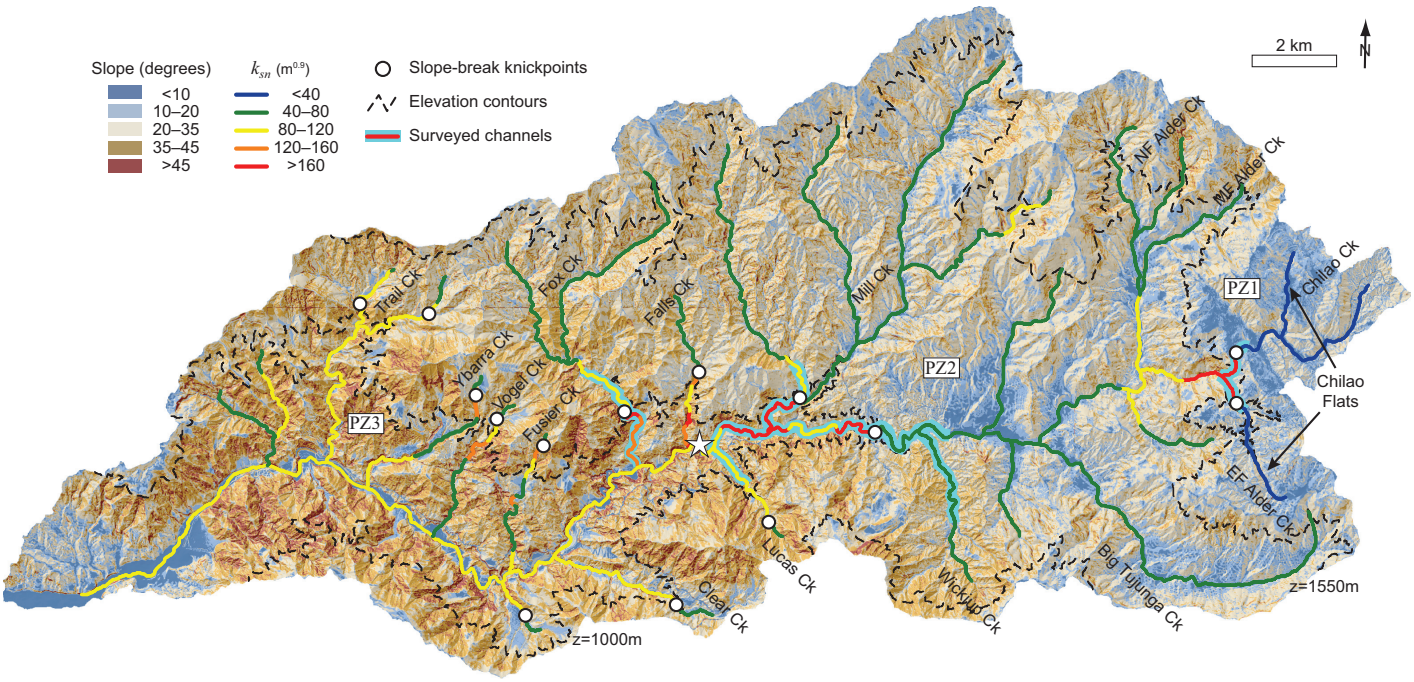

Figure 4. Overview of Big Tujunga Creek, showing hillslope angle overlain by stream network color coded by channel steepness index. Dashed lines indicate elevation contours of 1000 m and 1550 m, which roughly delineate three physiographic zones (PZ1–PZ3) within the basin. White star indicates location of Figures 5 and 13. EF—East Fork; MF—Middle Fork; NF—North Fork.

profiles at the locus of base-level fall, and E_1 is the erosion rate of the uppermost channel segment (PZ1). Profiles were projected following Equation 2, assuming a static drainage network (Schoenbohm et al., 2004). We used a fixed reference concavity index (θ_{ref} = 0.45) and extrapolated profiles using the average k_{sn} of each upstream, relict channel network. These reconstructions make no assumptions regarding erosion process and depend only on the accuracy of projected river profiles and the locus of baselevel fall (i.e., active fault), an assumption of uniform uplift (i.e., minimal tilting), and measurements of either rates of rock uplift or river incision averaged over appropriate time scales.

For Big Tujunga Creek, determining ΔZ is straightforward if we assume changes in base level occur due to uniform block uplift along the Sierra Madre fault zone at the range front (Blythe et al., 2000). Projecting downstream the relict channel profiles of PZ1 and PZ2 results in values of ΔZ_{1-2} = 720 m and ΔZ_{2-3} = 200 m (Fig. 3). As described earlier herein, we used detrital ^{10}Be-derived estimates of the average erosion rates for each physiographic zone to determine E_1 = 45 ± 5 m/m.y.; E_2 = 165 ± 30 m/m.y.; and E_3 = 500 ± 200 m/m.y. Applying these values to Equations 4 and 5, we calculate ΔT_1 = 6.6 Ma (range: 5–8 Ma), and ΔT_2 = 0.6 Ma (range: 0.4–1.5 Ma).

The age of the upper slope-break knickpoint is relatively insensitive to the choice of E_3 and is consistent with independent estimates of the age of the Sierra Madre fault zone and initial San Gabriel Mountains uplift (Matti and Morton, 1993; Blythe et al., 2002). This suggests that PZ1 (Chilao Flats) is the last vestige of pre-uplift topography, analogous to the Big Bear Plateau in the San Bernardino Mountains (Spotila et al., 2002). The age and origin of the lower slope-break knickpoint are less clear due to uncertainties associated with the modern rate of base-level fall, E_3. Our results suggest a recent (<1 Ma) acceleration in slip rate along the southern range front, likely along either the Sierra Madre fault zone or the Vasquez Creek fault (Figs. 2 and 3). We hypothesize that this activity is related to the initiation of the right-lateral San Jacinto fault zone, which likely occurred ca. 1 Ma (Lutz et al., 2006; Kirby et al., 2007) to 1.8 Ma (Blisniuk et al., 2010). Morton and Matti (1993) speculated that the onset of activity on the San Jacinto fault zone led to accelerated reverse slip along the Cucamonga fault zone in the eastern San Gabriel Mountains, but the implications for the western San Gabriel Mountains are unclear. Recent work modeling crustal deformation constrained by global positioning system (GPS) station data in southern California (e.g., Meade and Hager, 2005; Marshall et al., 2009; Cooke and Dair, 2011) shows potential to elucidate the influence of slip transfer between the San Andreas and San Jacinto fault zones on the slip rates of the Sierra Madre and Cucamonga fault zones.

This tectonic framework calibrated to erosion rates determined from cosmogenic ^{10}Be data enables a test of how well the observed bedrock channel response matches the predicted transient behavior of detachment-limited stream-power models used for steady-state channels in the San Gabriel Mountains channels (DiBiase et al., 2010; DiBiase and Whipple, 2011). The transition between PZ2 and PZ3, at elevations near 1000 m, has previously been used as a type example for a channel network responding to a stepwise increase in rock uplift rate that broadly matches predictions from a linear stream-power model (Fig. 1A; Wobus et al., 2006a; Perron and Royden, 2013). We revisit this approach here with the aid of new 1-m-resolution LiDAR topographic data and field surveys to show that (1) the behavior of streams downstream of the knickpoints is inconsistent with stream-power models of incision due to the presence of numerous oversteepened knickzones and bedrock waterfalls; (2) slope-break knickpoints separating PZ2 and PZ3 are not evenly clustered near 1000 m, but increase in elevation downstream; and (3) the knickzone in the headwaters of Big Tujunga Creek separating PZ1 and PZ2 enhances the preservation of the pre-uplift relict landscape of Chilao Flats (Figs. 3–4).

METHODS

Topographic Analysis

We used two data sets for our topographic analysis: a 1-m-resolution DEM derived from airborne LiDAR, and a 10 m DEM from the U.S. Geological Survey (USGS) National Elevation Data set. We extracted channel long profiles of Big Tujunga Creek and its major tributaries from a merged LiDAR and USGS DEM resampled to a 5 m grid using the freely available channel profile toolbar for ArcMap and Matlab (www.geomorphtools.org). We reconstructed channel elevations influenced by the Big Tujunga dam and reservoir using pre-dam USGS topographic maps (50 ft [15.25 m] contour interval). For each profile, we used slope-area data to determine the normalized channel steepness index for individual reaches (0.5–5 km) using a fixed reference concavity $\theta_{ref} = 0.45$ (Wobus et al., 2006b). While there is some variability in the best-fit value of θ, particularly downstream of slope-break knickpoints, inspection of steady-state channel profiles using area-transformed distance-elevation plots, or chi plots (Perron and Royden, 2013; Willett et al., 2014), indicates a narrow range of acceptable reference concavities (θ ~ 0.4–0.5). The resulting long profiles and channel steepness maps facilitated the identification of prominent slope-break knickpoints that we interpret to mark the upstream extent of channel adjustment to local base-level change associated with the transitions from zone PZ1 to PZ2 and zone PZ2 to PZ3.

We used a 1-m-resolution LiDAR DEM for four tasks: (1) We made slope maps for visualizing channel and hillslope behavior across waterfalls and knickpoints; (2) we identified bedrock steps (waterfalls) taller than 3 m in channel profiles; (3) we mapped the extent of strath terraces identified in the field and from aerial imagery; and (4) we measured valley width for select channels (Fig. 5A). Slope maps were generated from the 1 m DEM based on the dip of a plane fit to a 3 × 3 window surrounding each pixel. By inspection, we identified waterfalls as channel segments steeper than 45° for at least 3 m in height along all channels draining areas greater than 0.5 km^2. For each identified waterfall, we extracted a local channel long profile across the step to determine height (Fig. 5A, inset). For surveyed channels that lie within the LiDAR coverage (Fig. 4), we calibrated this method based on field observations of channel-spanning bedrock steps, giving confidence that these steep sections (generally >50°) represent exposed rock rather than steep boulder reaches. We then transferred this map of bedrock steps to the channel long profiles to visualize and quantify the elevation drop composed of discrete steps compared to that from smoothly graded channel segments (Fig. 5A, inset).

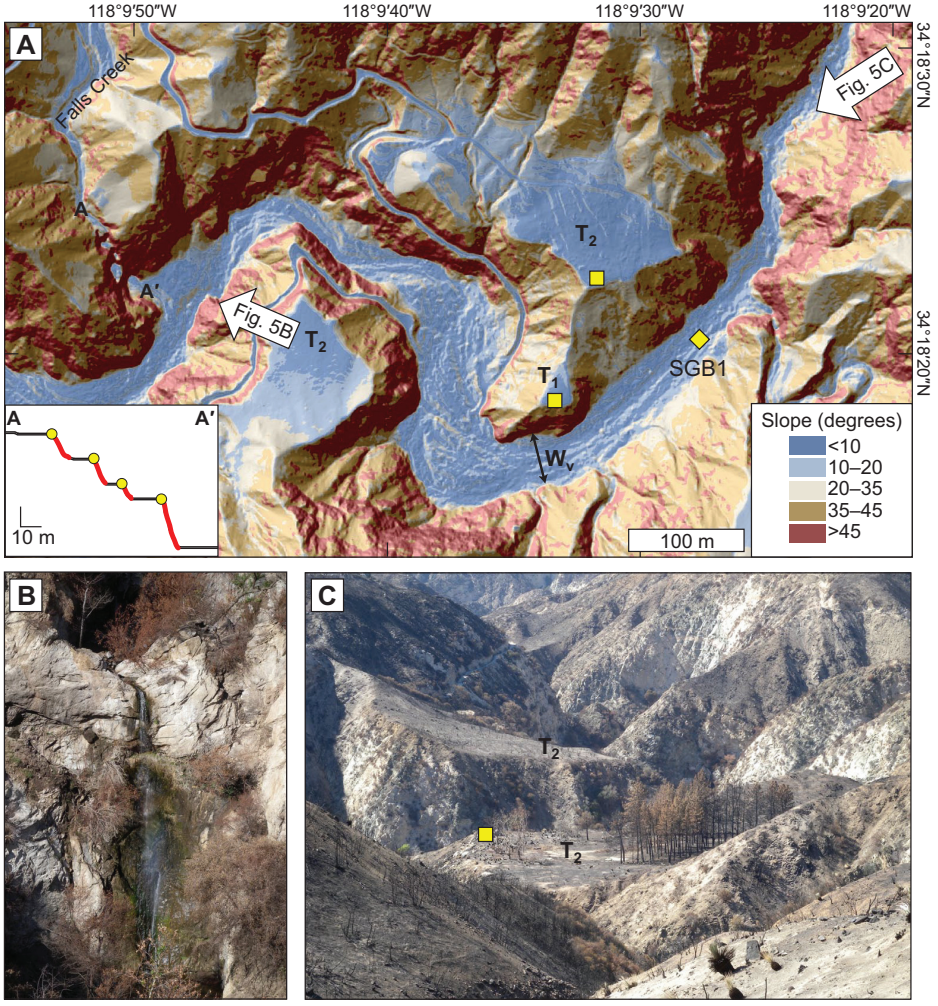

Figure 5. (A) Example of mapping morphologic features in the lower gorge of Big Tujunga Creek using 1 m light detection and ranging (LiDAR) slope map draped over shaded relief. Profile A-A′ (inset) shows a four-staged waterfall along Falls Creek, with bedrock steps shown in red with yellow circles. W_v indicates valley width as used in Figure 8. Strath terraces T_1 and T_2 appear as elevated low-sloping (<10°) regions adjacent to the main stem of Big Tujunga Creek. Block arrows show the location of photos (B) lower waterfall of Falls Creek and (C) terrace T_2 of Big Tujunga Creek (T_1 is out of view). Samples from terrace levels T_1 and T_2 are indicated by squares, and catchment sample SGB1 (DiBiase et al., 2010) is indicated by a diamond.

We also used the LiDAR slope map to identify regions of low (<10°) slope, which tend to correspond to valley flats and terraces. Terraces are readily identifiable along the lower reaches of Big Tujunga Creek, and occasionally in lower tributaries, but are rarely preserved in the upper reaches of the catchment (elevations >1000 m). Field observations indicate that these surfaces are predominantly strath (bedrock) terraces thinly mantled (~1–3 m) with alluvium (Fig. 5C). In addition to field observations, we used freely available low-altitude oblique aerial imagery taken after the 2009 Station Fire to identify alluvium-bedrock interfaces on strath terraces expressed in the LiDAR topography (www.bing.com/maps). We then transferred the mapped surfaces to the channel long profiles based on along-stream position and the elevation of the alluvium-bedrock interface. We determined the elevation of the alluvium-bedrock interface either by measurement in the field with a laser rangefinder, or by assuming a typical thickness of 2 m for the mantling alluvium.

Network Analysis of Knickpoint Retreat

In the absence of direct rate measurements, analyzing the relative migration patterns of slope-break knickpoints on tributaries within a single catchment (Crosby and Whipple, 2006; Berlin and Anderson, 2007), or on adjacent streams tied to a common base level (Whittaker and Boulton, 2012), enables the testing of bedrock incision laws. These area-dependent knickpoint celerity models have also been generalized and used to model waterfall migration rates, which are hypothesized to have similar network retreat patterns (Hayakawa and Matsukura, 2003; Bishop et al., 2005). To describe the network pattern of channel adjustment, we modeled waterfall and knickpoint retreat using a generalized celerity rule for which the horizontal retreat rate V_{kp} is a power-law function of drainage area A:

$$V_{kp} \propto A^{p}, \tag{6}$$

where p is an unknown exponent (e.g., Crosby and Whipple, 2006). Note that it is important to account for stepwise variations in drainage area as knickpoints migrate upstream (Crosby and Whipple, 2006; Whittaker and Boulton, 2012). Additionally, this treatment makes no assumption of incision process and simply describes the network behavior of a series of slope-break knickpoints or waterfalls. Within this framework, the relative elevation pattern of knickpoints depends on the relative magnitudes of the exponent p and the concavity index θ of the upstream relict stream network (Eq. 2), purely from geometrical considerations; for $p > \theta$, knickpoint elevations increase upstream; for $p < \theta$, knickpoint elevations decrease upstream; and for $p = \theta$, knickpoints lie at the same elevation (similar to predictions from stream-power incision models). However, while the case of equal-elevation knickpoints ($p = \theta$) is often invoked as a test of detachment-limited stream-power response (e.g., Niemann et al., 2001; Wobus et al., 2006b), this behavior is sensitive to assumptions of the uniform channel steepness and concavity of relict stream networks, which varies in natural landscapes. These variations are typically overlooked, but herein we illustrate how even moderate scatter (±10%) in the initial channel steepness index can introduce significant variability to the predicted location of slope-break knickpoints in the channel network.

Channel Surveys

To supplement our DEM analysis with observations of channel bed morphology, bed state, and details of channel form (e.g., presence of waterfalls and strath terraces), we surveyed ~20 km of nine channels in the Big Tujunga Creek watershed, including the main stem across its slope-break knickpoints, and multiple smaller side tributaries that enter the lower gorge (Fig. 4). We used a laser rangefinder and electronic data logger to geolocate measurements of bed cover and channel geometry at intervals of 20–50 m. We estimated the percent of bedrock exposed in channel bed and banks to the nearest 10% and measured bankfull width based on vegetation lines and high flow marks. In reaches with extensive valley flats (width >20 m), field surveys were supplemented with measurements of valley width from the 1 m LiDAR DEM (Fig. 5A). At each survey location, the median grain diameter of bed material (D_{50}) was estimated by eye, with periodic calibration using pebble counts of 100 grains—typically once every 1–2 km surveyed. Additionally, we noted channel-spanning bedrock steps taller than 3 m, and identified strath terrace surfaces where visible from the channel, all of which are in strong agreement with interpretations based on the LiDAR DEM analysis.

We used our survey data to quantify patterns of sediment transport stage across slope-break knickpoints in conjunction with LiDAR topographic data and historical streamflow records. For steady-state channels in the San Gabriel Mountains, DiBiase and Whipple (2011) estimated that floods overcoming initial-motion thresholds of bed material have a return interval of ~1 yr, and we use this flood to estimate the relative degree of bed mobility. We calculated bed shear stress τ associated with the 1 yr recurrence interval flood as:

$$\tau = k_t \left(\frac{Q_1}{w}\right)^{\alpha} S^{\beta}, \tag{7}$$

where $k_t = \rho g^{2/3} f^{1/3}/2$ is a constant that incorporates gravitational and frictional terms, Q_1 is the 1 yr recurrence interval flood, w is bankfull channel width measured from field surveys, S is channel slope, α and β are exponents that depend on the frictional relationship used (Howard et al., 1994), g denotes gravitational acceleration, and ρ is water density. We assume a Darcy-Weisbach friction factor $f = 0.08$ ($k_t = 1000$ m$^{-7/3}$ s$^{-4/3}$ kg and $\alpha = \beta = 2/3$) for all reaches based on typical values for gravel-bedded rivers (Parker et al., 2007). Frictional losses in boulder-bedded reaches are likely much greater, but we lack data to quantify this variation. We determined Q_1 for each reach based on a robust linear fit between Q_1 (m^3/s) and A (km^2) determined from mean daily runoff data across the San Gabriel Mountains ($Q_1 = 1.8A$; DiBiase and Whipple, 2011). Slope is based on a 200 m moving average calculated from channel long profiles extracted from LiDAR 1 m topographic data. We determined the nondimensional Shields stress τ^* according to:

$$\tau^* = \frac{\tau}{(\rho_s - \rho) g D_{50}}, \tag{8}$$

where ρ_s is sediment density (2650 kg/m^3). We calculated transport stage (τ^*/τ^*_c) using a slope-dependent critical Shields stress for incipient motion $\tau^*_c = 0.15S^{0.25}$, which ranges from 0.03 to 0.13 (Lamb et al., 2008b).

Cosmogenic ^{10}Be Dating of Terrace Surfaces

To provide an independent control on the retreat rate of lower Big Tujunga Falls (Fig. 3), we measured in situ–produced cosmogenic ^{10}Be concentrations of alluvium mantling two adjacent strath terraces along the main stem of lower Big Tujunga Creek (T_1 and T_2: 35 m and 54 m above the modern channel, respectively; Fig. 5). In total, we collected five amalgamated samples consisting of 1–2-cm-thick surface chips from the largest (1–2 m diameter) and best-preserved boulders on each surface. The sampled boulders are similar in appearance to boulders found in the modern stream channel, and they are located at the streamwise edge of the terraces, away from potential colluvial deposition influences. Thus, we interpret the boulder ages to reflect the abandonment of the terraces plus any prior inherited signal (Anderson et al., 1996). We isolated 50–100 g of quartz from each sample at Arizona State University following standard methods (Kohl and Nishiizumi, 1992), and ^{10}Be/^{9}Be ratios were measured on the accelerator mass spectrometer at PrimeLab (Purdue University). We calculated production rates and converted ^{10}Be concentrations to exposure ages or erosion rates using the CRONUS calculator (Balco et al., 2008) and corrected for topographic shielding using the 1 m LiDAR DEM.

RESULTS AND ANALYSIS

In contrast to models that predict smooth transitions between reaches of differing channel steepness index (e.g., Fig. 1A), slope-break knickpoints along Big Tujunga Creek lie at the head of oversteepened knickzones containing waterfalls. In total, we identified over 800 individual waterfalls taller than 3 m along the main stem and tributaries ($A > 0.5$ km^2) of Big Tujunga Creek. In this section, we present the results and analysis organized according to three prominent knickpoints and associated knickzones identified along the main stem of Big Tujunga Creek. The upper knickpoint refers to the prominent

slope-break along Chilao Creek at an elevation of ~1550 m (Figs. 3 and 6). The middle knickpoint refers to the slope-break along the main stem of Big Tujunga Creek at ~950 m, along with corresponding slope-break knickpoints along tributaries at elevations ranging from 900 to 1200 m (Figs. 3 and 7). The lower knickpoint corresponds to Lower Big Tujunga Falls and its associated knickzone at an elevation of ~800 m along the main stem (Figs. 3 and 7).

Upper Knickpoint (Chilao Creek)

The upper knickpoint in Big Tujunga Creek, separating PZ1 and PZ2, is confined to Chilao Creek and the East Fork of Alder Creek (black lines, Fig. 6). Low-gradient streams (S ~0.02; k_{sn} = 18–22 $m^{0.9}$) draining Chilao Flats are separated from steeper downstream reaches (S ~0.03; k_{sn} = 65 $m^{0.9}$) by a greatly oversteepened, 275-m-high knickzone (S ~ 0.3; k_{sn} = 390 $m^{0.9}$). The knickzone on Chilao Creek consists of a series of 15 waterfalls, which make up 45% of the total channel relief (125 m out of 275 m). Removing the elevation drop due to waterfalls, the channel steepness index of the knickzone (k_{sn} = 220 $m^{0.9}$) is still higher than the maximum observed steady-state channel steepness index (k_{sn} = 180 $m^{0.9}$) within the San Gabriel Mountains (DiBiase et al., 2010). In contrast to Chilao Creek, the adjacent tributaries of Alder Creek (gray lines, Fig. 6) and Mill Creek do not contain slope-break knickpoints, have few waterfalls, and are well characterized by a single channel steepness value throughout their length (k_{sn} ~ 64 $m^{0.9}$).

Field surveys of Chilao Creek reveal systematic changes in channel conditions associated with knickzone steepening (Fig. 8). Valley width decreases downstream from 80 m to a minimum of 8 m at the head of the knickzone, and then increases gradually to 30 m (Fig. 8F). The width of the active channel is difficult to measure due to large boulders that mantle the steepened reach, but we do not see evidence for channel narrowing across the knickpoint. Rather, there is a slight widening that appears to be associated with an increase in bed material size. Bedrock exposure in the bed and banks

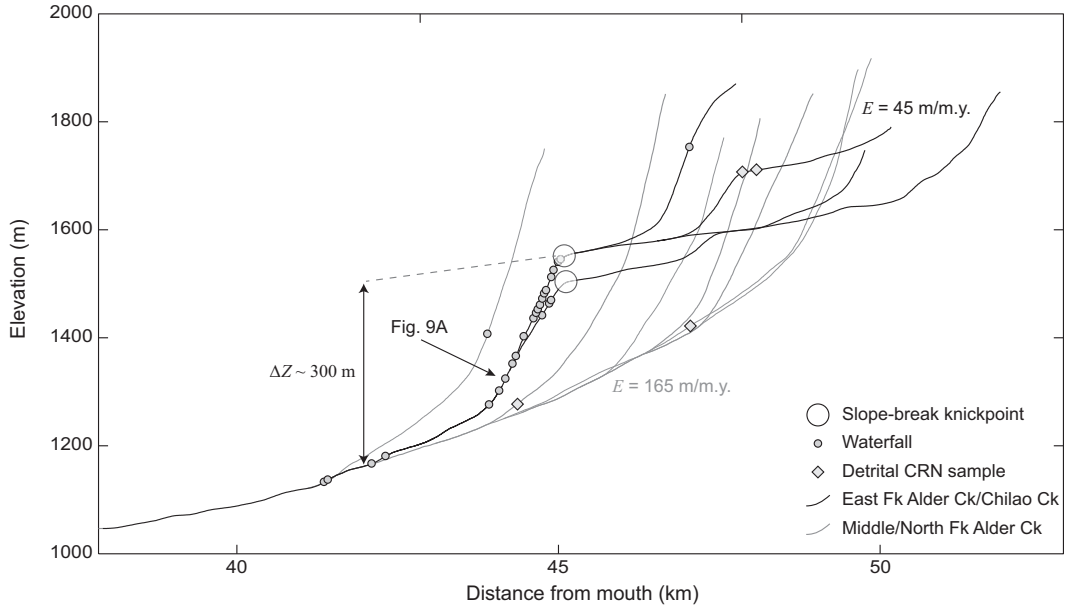

Figure 6. Long profiles of Alder Creek and Chilao Creek (upper knickpoint) highlighting role of waterfalls (small gray circles) in preserving relict stream profiles. Gray profiles correspond to the Middle and North Forks of Alder Creek, while the black profiles correspond to the East Fork of Alder Creek and Chilao Creek (Fig. 4). Arrows indicate incision of Alder Creek relative to the projected long profile of Chilao Creek (dashed line). Mean erosion rate *E* for PZ1 and PZ2 determined from detrital cosmogenic radionuclide (CRN) analysis is shown for reference.

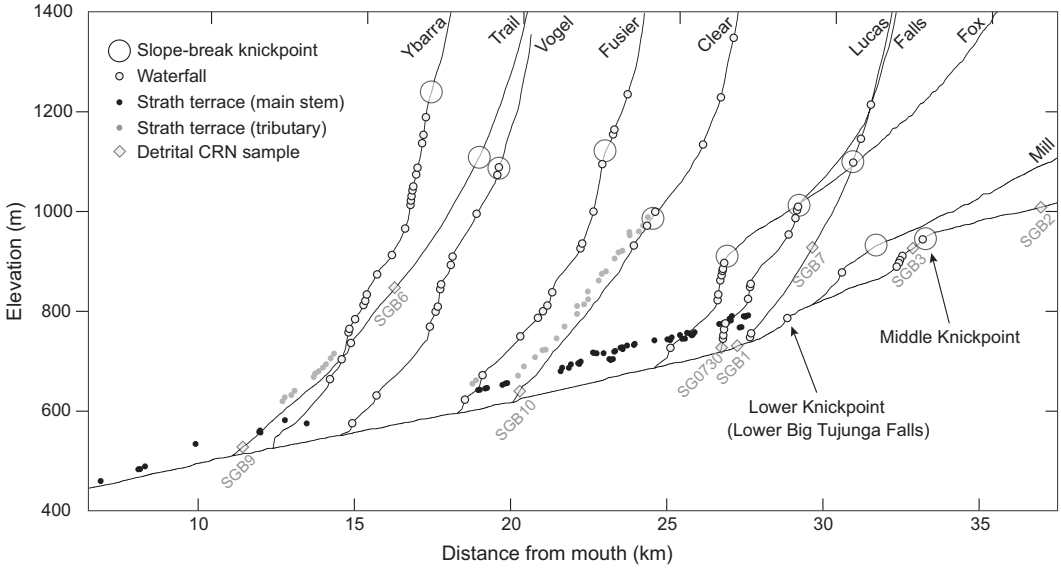

Figure 7. Lower Big Tujunga Creek tributary long profiles highlighting slope-break knickpoints (large white circles), strath terraces on tributary (gray dots), and main-stem channels (black dots), waterfalls (small circles), and locations of catchment-averaged erosion rates determined from cosmogenic radionuclide (CRN) analysis (sample numbers refer to DiBiase et al., 2010).

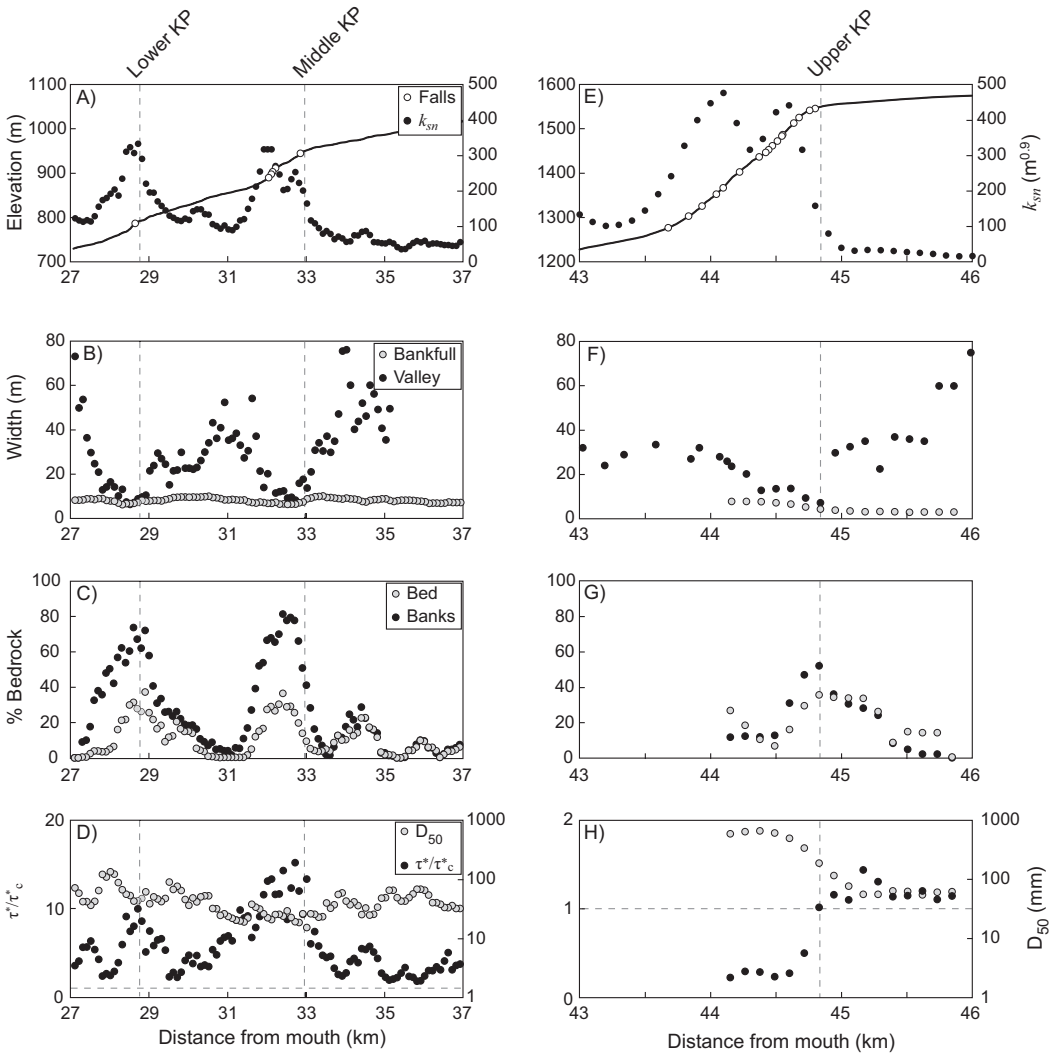

Figure 8. Summary of field channel survey data for (A–D) lower Big Tujunga Creek and (E–H) Chilao Creek. Vertical dashed lines indicate location of knickpoints (KP) highlighted in Figure 4. Horizontal dashed lines in D and H indicate initial motion threshold ($\tau^*/\tau^*_c = 1$).

also varies inversely with valley width, and the reach with the highest in-channel bedrock exposure is located just upstream of the knickzone (Fig. 8G). Bedrock exposure in the bed and banks decreases as Chilao Creek steepens and corresponds with a large increase in grain size from gravel to large boulders sourced from adjacent bedrock hillslopes (Fig. 8H). Calculations of bed-load transport stage associated with a 1 yr recurrence interval flood are just above critical upstream of the knickpoint and decrease to below incipient motion thresholds downstream despite increased channel slopes, due to this 10-fold increase in grain size (Fig. 8H).

Qualitative field observations from downstream of the surveyed reach indicate continued patchiness of bare bedrock and boulders in the channel bed, but very little bedrock confinement in banks (Fig. 9). The hillslopes lining the knickzone on Chilao Creek do not form an inner gorge, and there are no preserved strath terraces. Instead, the location of waterfalls in the channel lines up with bands of less-fractured and more-resistant bedrock on the hillsides (Fig. 9B), indicating that the hillslopes have had sufficient time to adjust to local channel incision rates. The waterfalls in Chilao Creek are characterized by vertical faces of massive granite that show near-horizontal jointing patterns that are expressed in adjacent hillslopes (Fig. 9A). Bedrock plunge pools at the base of these waterfalls are either shallow or absent.

Waterfall Retreat Rates

While there are no direct measurements of waterfall retreat rates on Chilao Creek, we can use cosmogenic erosion rates and tributary channel long-profile analysis to estimate the time scale for the growth of the knickzone, and in turn a maximum retreat rate for waterfalls at the head of this reach. Relative to the Chilao slope-break knickpoint, the main stem of Alder Creek has incised ~300 m (Fig. 6). The difference in catchment-averaged erosion rate measured with detrital ^{10}Be between Chilao Creek (E = 45 m/m.y.) and samples from the Middle and North Forks of Alder Creek (E = 165 m/m.y.; DiBiase et al., 2010) implies an age of 2.5 Ma (Eq. 4), and thus a maximum retreat rate of ~1 mm/yr if the entire knickzone has retreated 3 km from the confluence of Chilao Creek and the main stem of Alder Creek over this same time. However, average rates of vertical bedrock hillslope lowering measured in the Alder Creek catchment are less than 0.1 mm/yr and imply horizontal retreat rates of less than 0.2 mm/yr for a slope of 30° (Heimsath et al., 2012). Based on the

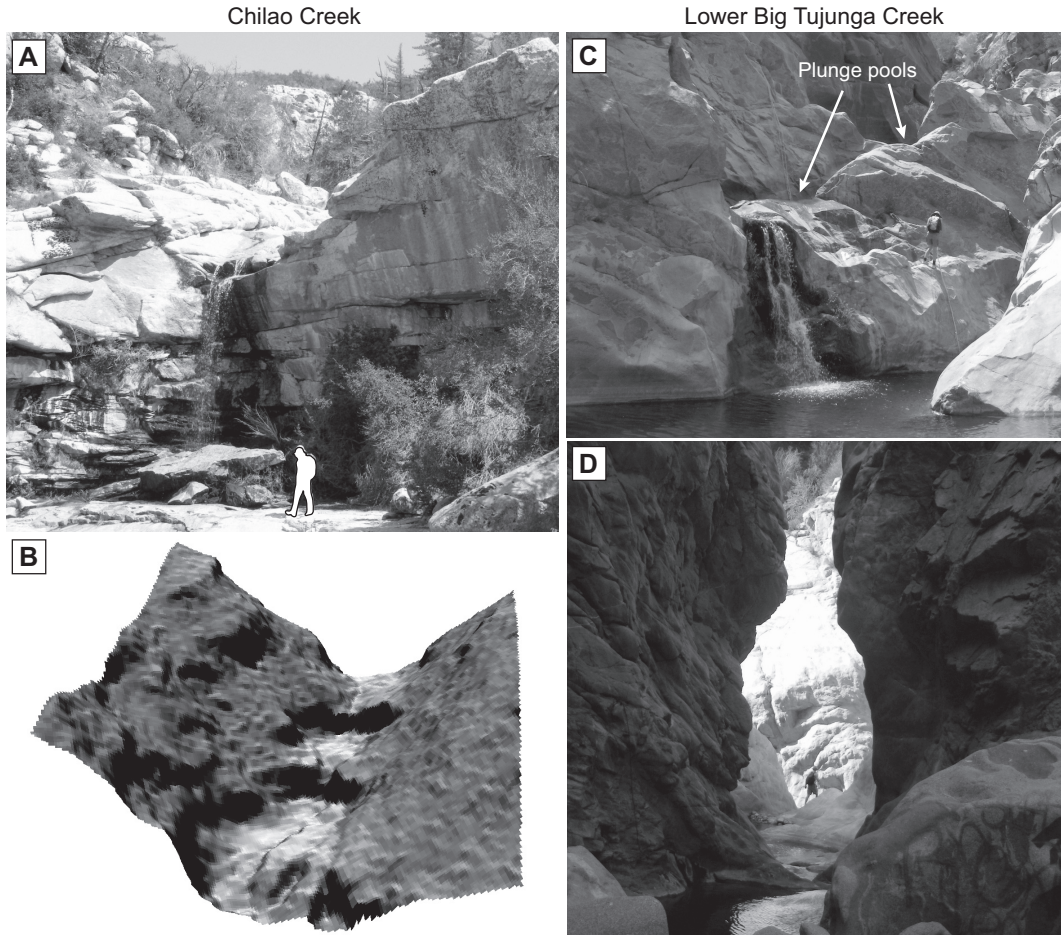

Figure 9. Field observations of waterfall and associated hillslope morphology. Waterfalls in Chilao Creek (A) tend to be blocky, lack inner gorges and plunge pools, and merge with hillslope bedrock outcrops, as observed in 1 m light detection and ranging (LiDAR) topography (B). Perspective slope map in B is centered on the waterfall in panel A, with darker colors corresponding to steeper slopes. Waterfalls in lower Big Tujunga Creek downstream of the middle slope-break knickpoint tend to have sculpted plunge pools (C), and leave a wake of oversteepened hillslopes that form narrow inner gorges, as seen downstream of Lower Big Tujunga Falls (D).

similarity in hillslope form and lack of relative incision, we hypothesize that the rates of waterfall retreat on Chilao Creek and the East Fork of Alder Creek are similarly of order 0.1 mm/yr.

Interpretation

We interpret that the preservation of Chilao Flats has been enabled by the waterfalls and associated boulder-mantled reaches slowing slope-break knickpoint retreat along Chilao Creek. The oversteepened knickzone along Chilao Creek is typical of vertical erosion rates (and corresponding values of V_{kp}) much greater than 1 mm/yr (DiBiase et al., 2010), yet waterfall retreat rates appear to be at least an order of magnitude slower. In contrast, evidence for the equivalent relict landscape has been eroded on the Middle and North Forks of Alder Creek (Fig. 6). On these tributaries, the upper slope-break knickpoint has already passed through the channel network (a distance of ~7.5 km), indicating a minimum V_{kp} of 3 mm/yr averaged over the past 2.5 m.y.

These results are consistent with the conceptual model of a slow knickzone (Fig. 1C), in that Alder Creek downstream of the Chilao knickzone grades smoothly with adjacent tributaries that do not contain waterfalls or slope-break knickpoints. If the Chilao waterfalls were fast, we would expect to see a downstream reach that is less steep than its final steady-state slope (Fig. 1B). Instead, Alder Creek and Big Tujunga Creek downstream of the Chilao oversteepened reach have similar channel steepness to the surrounding, adjusted channels (k_{sn} ~65 $m^{0.9}$). Furthermore, detrital ^{10}Be-based erosion rates from the adjusted tributaries (Middle and North Forks of Alder Creek) are consistent with rates measured throughout the intermediate physiographic zone (165 m/m.y.) and more than three times higher than rates from Chilao Flats (45 m/m.y.; DiBiase et al., 2010), implying that the upper slope-break knickpoint indeed represents a temporal change in base level and not simply a spatial variation in rock strength (Whipple et al., 2013). While the adjusted tributaries of Alder Creek are graded to the base level of PZ2 (sharing both similar topography and erosion rates), Chilao Flats (PZ1) has been insulated from changes in base level lower in Big Tujunga Creek by the waterfalls and boulder-mantled reaches of the Chilao knickzone. Because waterfalls in the Chilao knickzone are continuous with bands of bedrock exposed along hillslopes, we hypothesize that these waterfalls are exhumed, structurally controlled features that experience little to no headward migration. Thus, while the individual waterfalls do not likely change in height, continued downstream base-level lowering increases the overall height of the knickzone with time (Fig. 1C).

Middle Knickpoint

The middle knickpoint of Big Tujunga Creek delineates PZ2 and PZ3 and, like the upper knickpoint on Chilao Creek, lies at the head of an oversteepened (S ~0.06, k_{sn} ~250 $m^{0.9}$), waterfall-rich knickzone. The middle knickzone contains five waterfalls that account for 30% of the total channel relief on the main stem (21 m out of 70 m); however, the morphology of waterfalls and intervening channel reaches downstream of the middle knickpoint share little in common with the knickzone of Chilao Creek. First, in contrast to Chilao Creek, the middle knickzone waterfalls have deep plunge pools and fluvially sculpted bedrock (Fig. 9C), and

the locations of waterfalls do not appear to be structurally or lithologically controlled. Second, field surveys of Big Tujunga Creek spanning the middle knickpoint show different trends from Chilao Creek. The reach just upstream of the middle knickpoint is characterized by a gradual steepening and increase in bedrock exposure, as observed in many other landscapes (Haviv et al., 2006; Berlin and Anderson, 2009; Valla et al., 2010). As the channel steepens downstream of the slope-break knickpoint, valley width and channel width decrease (Fig. 8B), and bedrock exposure increases in the channel bed and banks (Fig. 8C). In contrast to Chilao Creek, increases in grain size across steepened reaches are subdued. Although boulders associated with local collapse of inner gorge faces or waterfall retreat are common, the active channel is predominantly mantled by cobbles and finer material. As a result, the calculated transport stage associated with a 1 yr recurrence interval flood increases across steepened reaches to well above incipient motion thresholds (Fig. 8D).

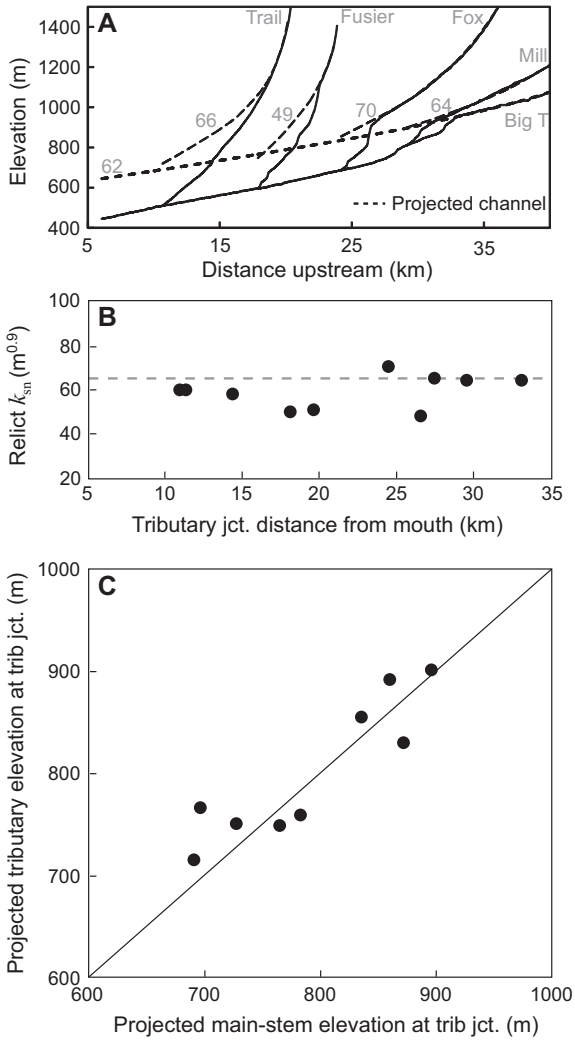

Figure 10. Plots characterizing concordance of upland (relict) stream network of tributaries to lower Big Tujunga Creek. (A) Projections of select tributary and main-stem relict channels (dashed lines). Gray numbers indicate value of relict channel steepness index (units of $m^{0.9}$). (B) Upstream of their slope-break knickpoints (white circles, Fig. 7), tributary channel networks have similar channel steepness index values (60 ± 10 $m^{0.9}$), which we interpret to correspond to PZ2. Horizontal dashed line indicates mean k_{sn} for PZ2 (64 $m^{0.9}$). (C) Projections of relict main-stem and tributary channel profiles at tributary junctions (jct.) are at similar elevations, and in lower Big Tujunga Creek define the continuous paleolandscape of PZ2.

Network Patterns of Knickpoint Retreat

While the upper knickpoint of Big Tujunga Creek is only preserved in one localized area (Chilao Creek and East Fork Alder Creek), all major tributaries to the lower reaches of Big Tujunga Creek contain slope-break knickpoints that we and others (Wobus et al., 2006a; Perron and Royden, 2013) interpret to be correlative to the middle knickpoint (Figs. 3 and 7). Above their slope-break knickpoint, these tributaries are characterized by a moderately steep upper reach (k_{sn} = 50–70 $m^{0.9}$) that is characteristic of PZ2 (Figs. 10A and 10B). Using the best-fit k_{sn} of the relict channel, we projected tributary long profiles downstream to their junction with the main-stem Big Tujunga Creek assuming a concavity index $\theta = 0.45$ (Fig. 10A). The agreement in elevation between the projections of tributary relict channels and a similar projection of the main-stem Big Tujunga Creek downstream of its middle knickpoint indicates a continuous pre-incision tributary network that defines PZ2, and corresponds to a relative base-level drop of ~200 m relative to the current range-front elevation (Figs. 3 and 10A). Downstream of their main slope-break knickpoint, tributaries show contrasting behavior. For example, Lucas Creek and Clear Creek have few bedrock steps along their length (7% and 3% of relief below knickpoint), while Fox Creek and Falls Creek drop from their upstream reaches to the lower gorge of Big Tujunga Creek via a series of 10–30 m waterfalls (~40% of relief below knickpoint; Table 1). In general, tributary channels become less incised with distance upstream of Big Tujunga Creek; however, Fox Creek and Mill Creek exhibit dramatic inner gorges with

TABLE 1. BIG TUJUNGA CREEK TRIBUTARY SLOPE-BREAK KNICKPOINT PARAMETERS (MIDDLE KNICKPOINT)

Stream name	Area (km^2)	DFM (km)	X_{kp} (km)	Z_{kp} (m)	Relict k_{sn} ($m^{0.9}$)	Z_{proj} trib (m)	Z_{proj} Big Tuj. Ck (m)	Total WF height (m)	WF relief fraction
Trail	17	10.7	7.9	1110	66	715	690	14	0.02
Ybarra	5	12.0	5.8	1232	56	765	695	218	0.31
Vogel	5	14.1	5.1	1085	50	750	726	148	0.28
Fusier	3	17.9	4.7	1121	49	748	765	96	0.18
Clear	8	19.6	4.3	975	52	758	782	11	0.03
Fox	25	24.2	2.3	907	70	855	836	92	0.42
Falls	6	26.3	2.5	1010	49	893	860	115	0.40
Lucas	4	27.2	3.4	1103	67	830	871	27	0.07
Mill	57	29.2	1.9	925	64	901	896	8	0.07

Note: DFM—tributary junction distance from mouth; X_{kp}—streamwise retreat distance of slope-break knickpoint from main-stem Big Tujunga Creek; Z_{kp}—elevation of slope-break knickpoint; Z_{proj}—elevation of projected tributary or main-stem relict channel at confluence with Big Tujunga Creek; total WF height—sum of individual waterfall heights downstream of slope-break knickpoint on each tributary; WF relief fraction—total waterfall height divided by tributary relief downstream of slope-break knickpoint.

fluvially sculpted and undercut bedrock walls immediately downstream of their slope-break knickpoints.

In contrast to predictions from stream-power–type incision models and prior analysis (Wobus et al., 2006a), we find that the elevations of slope-break knickpoints on tributaries increase with distance downstream of the middle knickpoint on Big Tujunga Creek and vary in elevation from 900 to 1200 m (Fig. 11A). Taken at face value, the pattern of planform knickpoint retreat is best fit by a celerity model (Eq. 6) with an area exponent $p = 0.33$ (Fig. 11C), which is less than the concavity index of the upland (PZ2) stream network ($\theta \sim 0.45$), and consistent with the pattern of slope-break knickpoint elevations increasing downstream. Surprisingly, there is no clear relationship between retreat distances normalized by the best-fit drainage area dependence and the number or size of knickzones or waterfalls present (Table 1).

Interpretation

The network distribution of slope-break knickpoints associated with the middle knickpoint indicates that these are retreating features, but the influence of waterfalls and knickzones on the retreat rate of these slope-break knickpoints is unclear, despite the systematic deviation from the stream-power prediction of uniform knickpoint elevation (Niemann et al., 2001). Two factors complicate a straightforward interpretation of how waterfalls and knickzones influence landscape adjustment associated with the middle knickpoint on the main stem and tributary channels.

First, unlike the upper knickpoint on Chilao Creek, all tributaries draining into lower Big Tujunga Creek have slope-break knickpoints along their profile (Fig. 7), and thus, we do not know a priori the steady-state channel steepness index expected for the modern uplift rate at the range front. This precludes a simple evaluation relative to the channel steepness index of the main stem downstream of the knickzones (k_{sn} ~80 $m^{0.9}$). Instead, we used our estimate of E_3 (500 ± 200 m/m.y.) to evaluate the landscape morphology relative to the robust relationship developed for steady-state channels elsewhere in the San Gabriel Mountains (DiBiase et al., 2010). These rates are typically associated with normalized channel steepness values of 110 $m^{0.9}$ or higher, and they suggest that Big Tujunga Creek downstream of the middle knickzone is less steep than expected, and in agreement with predictions for fast knickzone retreat (Fig. 1B).

Second, the expectation of uniform slope-break knickpoint elevation on tributaries relies on the assumption of uniform channel steepness and concavity indexes for upstream relict stream networks. Although the tributaries to lower Big Tujunga Creek draining PZ2 are broadly similar (mean $k_{sn} = 60 \pm 10$ $m^{0.9}$) and project onto a continuous network with the main stem (Fig. 10A), even these slight variations in upstream channel steepness can introduce large variations in predicted slope-break knickpoint elevation. Additionally, the predicted slope-break knickpoint elevations become increasingly sensitive to these deviations as they reach steep headwater reaches. Thus, if there were systematic trends in the steepness of relict channels with distance upstream, a spurious trend in knickpoint elevation could emerge. To test this, we modeled the predicted location of slope-break knickpoints for tributaries of Big Tujunga Creek assuming a detachment-limited stream-power model where the adjusting channels have a constant steepness index. We used a value of $k_{sn} = 102$ $m^{0.9}$, as this value both predicts the location of the middle knickpoint on the main-stem Big Tujunga Creek and roughly corresponds to the expected steady-state steepness associated with E_3 ~500 m/m.y. If the upstream channel network had a uniform $k_{sn} = 62$ $m^{0.9}$ (corresponding to the k_{sn} of the main-stem Big Tujunga Creek above the middle knickpoint), then the tributary slope-break knickpoint elevations would lie at a constant elevation of ~955 m. However, the variations in relict channel steepness of tributaries to lower Big Tujunga Creek, even though they are not systematic (Fig. 10B), result in predicted slope-break knickpoint elevations of 850–1050 m (Fig. 11A).

Overall, it appears that the middle knickpoint represents a case where some waterfalls and knickzones resulted in a net faster tributary slope-break knickpoint retreat rate (e.g., Fusier Creek), and some have resulted in a net slowing (e.g., Fox Creek). There is a rich diversity in waterfall morphology along knickzones, ranging from waterfalls with well-developed plunge pools in deeply incised inner gorges to unincised waterfalls that merge with hillslope bedrock exposure similar to those expressed in Chilao Creek. Yet, tributaries with few waterfalls or knickzones (e.g., Clear, Lucas, and Trail) do not seem to have fundamentally faster or slower relative knickpoint retreat rates than tributaries with significant waterfall-rich knickzones. Rather, we hypothesize that the details

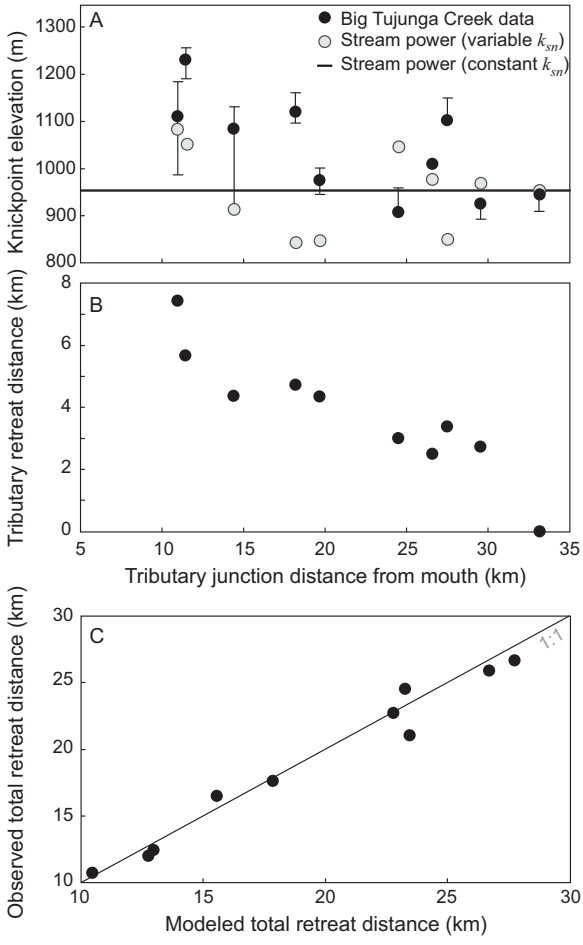

Figure 11. Network patterns of slope-break knickpoint retreat on tributaries to lower Big Tujunga Creek, showing knickpoint elevation (A) and migration distance from main-stem Big Tujunga Creek (B) against tributary junction distance from the range front. Zero retreat distance in B indicates the main-stem Big Tujunga Creek slope-break knickpoint. Error bars on points in A indicate streams with either multiple major tributaries or channel convexities that lack a definitive slope break. Horizontal line indicates constant knickpoint elevation predicted by stream-power models for constant relict and adjusting channel steepness index (k_{sn} = 62 $m^{0.9}$ and 102 $m^{0.9}$, respectively). Gray circles indicate knickpoint elevations predicted by stream-power models for variable relict channel steepness (Fig. 10B). (C) Plot showing agreement between observed and modeled slope-break knickpoint locations following a knickpoint retreat model where $V_{kp} \propto \mu A^{0.33}$.

of slope-break knickpoint retreat mechanisms are sensitive to local variations in lithology and sediment supply that are, at present, poorly constrained (see Discussion section). We interpret the general behavior of the middle knickpoint to be overall neutral, as we see evidence for both slow and fast behavior on individual tributaries, and our prediction for the location of the slope-break knickpoint following a calibrated stream-power–based model from the San Gabriel Mountains is within the spread of observed tributary slope-break knickpoint elevations.

Lower Knickpoint (Lower Big Tujunga Falls)

The lower knickpoint on the main stem of Big Tujunga Creek is defined by a 50-m-high knickzone ($S \sim 0.06$, $k_{sn} \sim 280\ m^{0.9}$) that offsets two lower-gradient reaches ($S \sim 0.02$–0.03, $k_{sn} \sim 80$–$110\ m^{0.9}$; Fig. 7). This knickzone is headed by Lower Big Tujunga Falls, a 7-m-high bedrock waterfall and plunge pool within a narrow and steep (in some places undercut) bedrock inner gorge (Fig. 9D). Downstream of Lower Big Tujunga Falls, two to three well-defined strath terrace levels extend 5 km downstream and are nearly parallel to the modern river channel (Fig. 7). Discontinuous strath terraces are preserved over an additional 15 km to the range-bounding Sierra Madre fault. Similar strath terraces that grade to the highest main-stem terrace level are well preserved on Trail Creek and Clear Creek, and to a lesser extent on other tributaries. Additionally, many tributaries enter the main stem of Big Tujunga Creek via waterfalls that are related to these strath terraces (e.g., Falls Creek; Fig. 5B).

Field surveys across the lower knickpoint show similar channel behavior as those spanning the middle knickpoint. Between upstream and downstream reaches mantled with alluvium, the lower knickzone shows a progressive channel and valley narrowing that is accompanied by a loss of sediment cover and increased bedrock exposure in channel bed and banks (Figs. 8B and 8C). Further downstream (downstream of the San Gabriel fault; Fig. 3), Big Tujunga Creek becomes increasingly alluviated, with inferred sediment depths approaching 100 m near the range front based on side-slope projections (Fig. 3). In the steepest reaches of the lower knickzone, channel width and valley width are equivalent, and Big Tujunga Creek is confined within a bedrock inner gorge (Fig. 9D). As observed across the middle knickpoint, bedload sediment does not significantly coarsen in the steep knickzone containing Lower Big Tujunga Falls (Fig. 8D).

Waterfall Retreat Rates

The ages and patterns of downstream strath terraces provide constraints on the retreat rate of Lower Big Tujunga Falls, which aligns with the uppermost strath terrace surface (T_2; Fig. 5). First, dating results from boulders mantling the two strath terrace levels indicate recent abandonment. Within error (1σ), cosmogenic ^{10}Be concentrations measured from the five boulder samples on two terrace levels are equivalent to each other and to ^{10}Be concentrations in modern stream sands collected nearby from the main stem of Big Tujunga Creek (Fig. 12; Table 2). Based on local production rates corrected for minimal topographic shielding, these concentrations correspond to an exposure age of 11 ± 4 ka (equivalent to 76 ± 27 m/m.y. steady erosion rate), and if the modern stream sands accurately represent the inherited ^{10}Be concentrations, the exposure age is zero within analytical error. While it is plausible that postdepositional weathering has decreased the ^{10}Be inventory of the sampled boulders, for example, via spallation associated with wildfire (Bierman and Gillespie, 1991), it is unlikely that enough erosion has occurred to account for the low measured concentrations. The most likely scenario is that the sampled terraces were both abandoned in the past 3–5 k.y. Based on these young exposure ages ~1 km downstream of Lower Big Tujunga Falls, we estimate an average retreat rate on the order of 200 mm/yr over the past few thousand years, which is of similar magnitude to rapid rates of waterfall retreat measured in other landscapes (e.g., Hayakawa and Matsukura, 2003; Lamb et al., 2007; Mackey et al., 2014). Although this retreat rate has large uncertainty associated with it, it is unlikely that the low ^{10}Be concentrations can be explained by a slowly (<1 mm/yr) retreating feature.

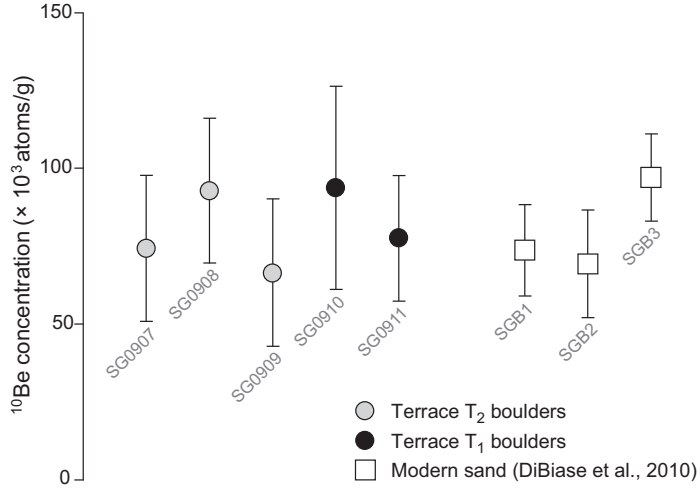

Figure 12. Comparison of ^{10}Be concentration measured from terrace boulders (Table 2) to concentrations measured in modern Big Tujunga Creek stream sands (DiBiase et al., 2010). Error bars indicate 1σ analytical error. Sample locations are shown in Figures 5 and 7.

TABLE 2. ^{10}Be DATA FROM TERRACE BOULDERS

Sample	Latitude (°N)	Longitude (°W)	Elevation (m)	Topographic shielding	^{10}Be concentration (10^3 atoms/g SiO_2)	Age (ka)	*E* (m/m.y.)
SG 09 07	34.3063	118.1588	790	0.985	74.3 ± 23.5	10.1 ± 3.3	82.5 ± 29.9
SG 09 08	34.3063	118.1588	790	0.985	92.8 ± 23.2	12.6 ± 3.4	65.4 ± 18.3
SG 09 09	34.3063	118.1588	790	0.985	66.5 ± 23.7	9.0 ± 3.3	92.5 ± 38.8
SG 09 10	34.3054	118.1591	770	0.975	93.7 ± 32.6	13.1 ± 4.7	63.5 ± 26.0
SG 09 11	34.3054	118.1591	770	0.975	77.6 ± 20.2	10.8 ± 3.0	77.4 ± 22.6

Note: Age—exposure age calculated assuming no erosion; *E*—erosion rate calculated assuming steady-state surface erosion. Calculations were made using the CRONUS calculator (Balco et al., 2008) with a sample thickness of 2 cm and density of 2.65 g/cm^3, following the constant production rate model of Lal (1991) and Stone (2000). ^{10}Be concentration is referenced to standard 07KNSTD.

Second, the geometry of abandoned strath terraces downstream of Lower Big Tujunga Falls is consistent with a rapidly retreating knickzone. Because the strath terrace level is parallel to the modern stream channel, the retreat rate of the lower knickzone and Lower Big Tujunga Falls must be fast relative to the background vertical incision rates of the upstream and downstream alluviated reaches (e.g., Finnegan, 2013). For comparison, the most rapid rates of long-term bedrock lowering in the San Gabriel Mountains are of order 1 mm/yr. It is less clear how this retreat rate compares with expectations from stream-power predictions of slope-break knickpoint retreat, as Lower Big Tujunga Falls and its knickzone do not represent a slope-break knickpoint because channel reaches upstream and downstream of the knickzone have similar channel steepness (Whipple et al., 2013).

As mentioned earlier herein, most tributary streams that enter the lower Big Tujunga gorge do so via waterfalls that are likely related to the abandonment of the strath terrace surface T_2 (Fig. 13A). Analysis of the network pattern of waterfalls on tributaries larger than 1 km^2 reveals these are retreating features tied to the migration of Lower Big Tujunga Falls (Fig. 13B). Notably, these waterfalls are retreating faster than the hillslope relaxation of the main-stem inner gorge, which we hypothesize to be due to waterfall erosion associated with observed well-developed plunge pools at the base of these falls. If we assume the retreat rate of Lower Big Tujunga Falls is constant at 200 mm/yr over the distance shown in Figure 13A, then the retreat rate of the tributary waterfalls ranges from 10 to 20 mm/yr, with higher rates generally corresponding to higher drainage area ($p \sim 0.5$; Fig. 13C). Thus, the network pattern of waterfall retreat appears to be consistent with knickpoint celerity models used for slope-break knickpoints (e.g., Bishop et al., 2005; Crosby and Whipple, 2006; Berlin and Anderson, 2007; Whittaker and Boulton, 2012).

Interpretation

Four lines of evidence point to rapid retreat of the lower knickzone including Lower Big Tujunga Falls. First, the pattern and ages of strath terraces downstream of the knickzone suggest rapid parallel retreat relative to background vertical channel incision (Fig. 7). Second, based on valley width measurements and a lack of observed in-channel bedrock, Big Tujunga Creek becomes increasingly alluviated downstream of its lowest oversteepened reach (Fig. 4), suggesting a channel less steep than expected by stream power at steady state, and consistent with predictions for fast knickzone retreat (Fig. 1B). Third, in contrast to Chilao Creek, the steepened reaches of lower Big Tujunga Creek between waterfalls are associated with channel narrowing (Fig. 8B), confinement by bedrock banks (Fig. 8C), and high in-channel bedrock exposure (Fig. 8C). As a result, the transport stage associated with the 1 yr flood increases across steepened reaches in lower Big Tujunga Creek and stays well above initial motion thresholds throughout its length (Fig. 8D). Throughout the San Gabriel Mountains, channels lacking slope-break knickpoints tend to be mantled with a thin veneer of alluvium and are likely close to transport-limited conditions (DiBiase and Whipple, 2011). Thus, up to a certain point, the decrease in sediment cover associated with the lower Big Tujunga Creek knickzone is expected to result in increased bedrock erosion until a transition to

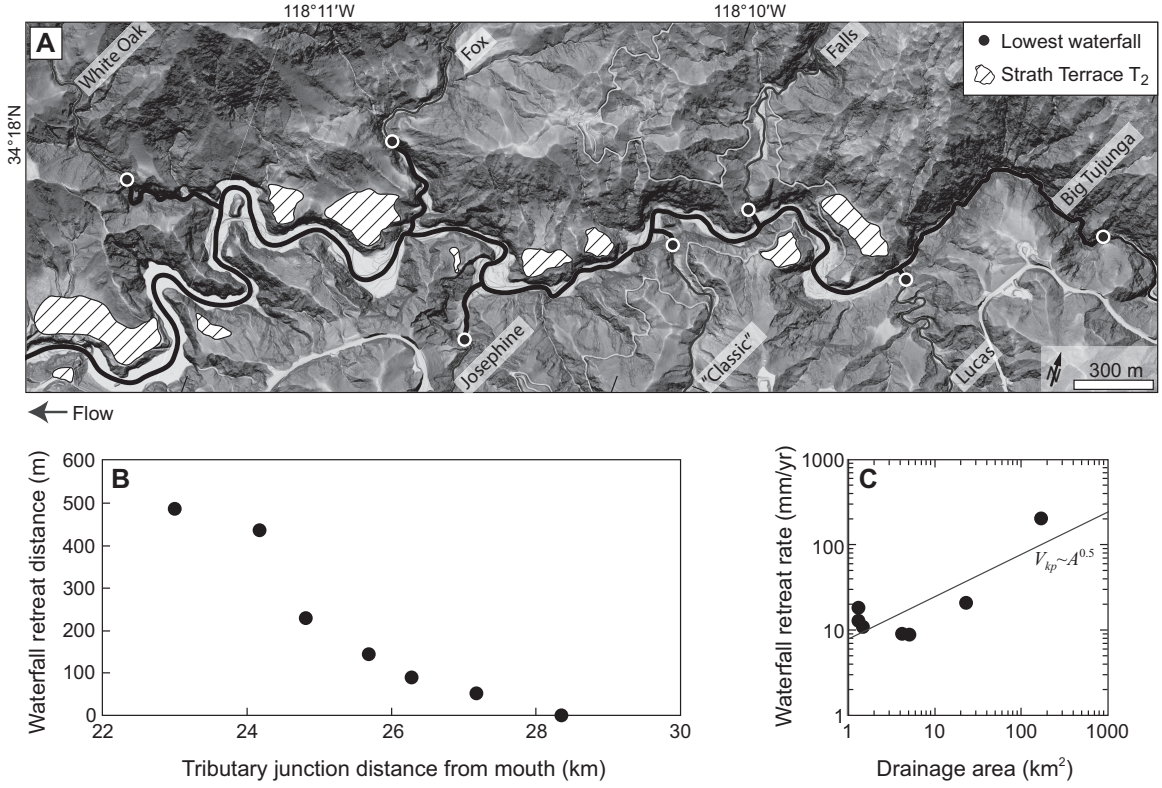

Figure 13. (A) Slopeshade map (darker shades—steeper slopes, lighter shades—terraces and alluvial fill) of lower Big Tujunga gorge showing distribution of strath terraces and associated waterfalls. Bold lines indicate distance of waterfall retreat from the main-stem Big Tujunga Creek (see part B). (B) Waterfall retreat distance from the main-stem Big Tujunga Creek versus distance upstream. (C) Plot of waterfall retreat rate against tributary drainage area, assuming constant retreat rate of 200 mm/yr for lower Big Tujunga Falls. Line shows fit to Equation 6 with $p = 0.5$.

tool-starved conditions is achieved (Sklar and Dietrich, 2004). Although river incision due to bed-load abrasion is predicted to decrease for high transport stages ($\tau^*/\tau^*_c > 10$) due to increasing saltation hop lengths (Sklar and Dietrich, 2004), extensive fluting of bedrock surfaces in lower Big Tujunga Creek suggests high erosion rates within the suspension regime (Hancock et al., 1998; Whipple et al., 2000; Hartshorn et al., 2002; Lamb et al., 2008a; Scheingross et al., 2014). Last, the waterfalls on the main stem of lower Big Tujunga Creek do not appear to be tied to lithologic contrasts and are associated with bedrock inner gorges consisting of side slopes that in places are vertical to undercut (Fig. 9), and relax downstream of oversteepened reaches (Gallen et al., 2011; Mackey et al., 2014). Bedrock exposure along the walls of inner gorges is extensive and unmatched in comparison to hillslopes elsewhere in the San Gabriel Mountains that are in balance with local channel incision rates (DiBiase et al., 2012; Heimsath et al., 2012).

Whereas the growth of the Chilao knickzone can be explained by the exhumation of more resistant bands of bedrock, the development of Lower Big Tujunga Falls requires a recent base-level drop on the order of 30–60 m, as indicated by the geometry of downstream strath terraces. Additionally, because the channel steepness upstream and downstream of the lower knickzone is similar, the lower knickpoint is unlikely to have been generated by a sustained increase in uplift rate, as we interpret to have occurred for the middle and upper knickpoints. Discrete changes in base level overprinted on longer-term forcings may occur due to large landslides (Ouimet et al., 2007), drainage reorganization (Yanites et al., 2013), or meander cutoffs (Finnegan and Dietrich, 2011), but we see no recent evidence for these factors, which would all leave a distinctive topographic signature on the landscape (there are numerous large landslides in the tributaries of Fusier and Ybarra Creeks, but these features appear unrelated to the recent base-level signal along the main stem). The magnitude of base-level drop is also larger than the estimated vertical slip for earthquakes on the range-bounding reverse faults (O[1 m]; Tucker and Dolan, 2001). Instead, we hypothesize that sudden base-level drop is driven by alluvial cut-and-fill cycles that periodically expose large bedrock steps formed from slip accumulated over multiple seismic events when the range-bounding faults are buried in sediment fill (e.g., Fig. 3). This mechanism is similar to that proposed by Finnegan and Balco (2013) to explain strath terrace formation in central California, but it has otherwise not previously been identified. In such a scenario, base-level lowering is accommodated by short-lived periods of rapid waterfall retreat rather than steady vertical channel incision (e.g., Seidl and Dietrich, 1992). Evidence for repeated aggradation, uplift, and incision in the form of entrenched and faulted fanheads is prevalent along the Sierra Madre–Cucamonga fault system (Eckis, 1928; Scott, 1973; Bull, 1991). In addition to climatic forcing, these cut-and-fill cycles may be internally driven by pulses of sediment flux following waterfall retreat, helping to explain the presence of multiple waterfalls and oversteepened reaches on both the main stem and tributaries of lower Big Tujunga Creek.

DISCUSSION

Controls on Waterfall Retreat Rates

Overall, analysis of the three major knickzones on Big Tujunga Creek indicates a progressive slowing of slope-break knickpoint retreat with increasing distance upstream. What drives the apparent four order-of-magnitude slowing of knickpoint retreat (~200 mm/yr to <0.2 mm/yr)? While the physics of waterfall erosion are poorly constrained and depend on the mechanism of retreat (e.g., plunge-pool drilling, undercutting, toppling, etc.), it is generally thought that the primary controls on waterfall retreat include rock strength and joint orientation, coarse sediment supply, and water discharge (e.g., Weissel and Seidl, 1997; Hayakawa and Matsukura, 2003; Lamb et al., 2007; Lamb and Dietrich, 2009; Haviv et al., 2010). We hypothesize that two factors, coarse sediment supply and local rock strength, act in concert to emphasize the differences in retreat rate observed in Big Tujunga Creek.

First, the availability of coarse sediment (gravel and cobbles) to abrade waterfall lips, drill plunge pools, and erode intervening non-waterfall reaches differs greatly within Big Tujunga Creek. For example, hillslope sediment supply to channels in the upper reaches of Chilao Creek is dominated by grus (typically coarse sand) and boulders produced from the weathered granitic surface of Chilao Flats. Boulders and bedrock in the Chilao Creek knickzone show some evidence for fine-scale abrasion and fluting, but overall, waterfall geometry is controlled by jointing, and plunge-pools are absent at the base of waterfalls (Fig. 9A). In contrast, rapidly eroding hillslopes deliver ample gravel- to cobble-sized material to the lower reaches of Big Tujunga Creek. Exposed bedrock in the bed and banks of lower Big Tujunga Creek are thoroughly sculpted and polished, and waterfalls are characterized by deep plunge pools (Fig. 9C). Whether this contrast is due primarily to network position (drainage area controlled) or to a difference in rock strength is unclear. However, fast waterfalls on Clear Creek and Trail Creek, as evidenced by their downstream strath terraces (Fig. 7), suggest that even waterfalls with catchments as small as a few square kilometers in the San Gabriel Mountains are capable of rapid retreat rates.

Second, there is a qualitative difference in the fracture density, and presumably strength, between bedrock exposed in the waterfalls and hillslopes of Chilao Creek and rock exposed in lower Big Tujunga Creek. At the landscape scale, rock strength variations in the San Gabriel Mountains do not appear to influence erosion rates significantly in areas not dominated by waterfalls (DiBiase et al., 2010). However, we see from the San Gabriel Mountains that in transient landscapes, waterfall retreat processes appear to be more sensitive to local heterogeneities. Along the escarpment adjacent to the Chilao Creek oversteepened reach, bedrock on hillslopes is exposed in structurally controlled bands that merge with in-channel waterfalls, and the location of waterfalls appears to be controlled by lithology (e.g., Ortega et al., 2013). In contrast, bedrock on hillslopes within lower Big Tujunga Creek is highly fractured and shows no clear structural trends. Waterfalls within lower Big Tujunga Creek do not necessarily align with rock exposures on hillslopes, and often there is evidence for significant recent migration (i.e., wake of strath terraces or inner gorge). We hypothesize that the fractured rock of lower Big Tujunga Creek both enables efficient drilling of plunge pools and inhibits the boulder-mantling of channels downstream of waterfalls as observed in Chilao Creek.

The interplay of rock strength, fracture density, and bed-load grain size likely exerts additional influence on local river incision and waterfall retreat rates that at present is difficult to quantify. These effects are most likely to be amplified where there is a difference between the local rock strength and the strength and caliber of bed load delivered from upstream sources. For example, the headwaters of Fox Creek and Falls Creek are composed of Precambrian anorthosite that rapidly declines in the coarse bed load as soon as sources for granitic cobbles emerge. Thus, the apparent slowing of the middle knickpoint and development of large waterfalls on these tributaries are likely enhanced by the contrast between weak bed load and strong in-channel bedrock. We hypothesize that the opposite case (strong bed load and weak in-channel bedrock) occurs in Clear Creek (Fig. 4), where the axis of the main channel follows the trace of the Quaternary San Gabriel fault (Fig. 2). Clear Creek has few

waterfalls and no major knickzones along its main stem (Fig. 7) but instead shows behavior consistent with detachment-limited stream-power incision (Fig. 1A). Refining models for waterfall and knickzone retreat will require continued field work to better quantify variations in hillslope and channel sediment supply and rock strength.

Implications for Landscape Evolution

Our results show that there is a clear break in behavior between steady-state and transient bedrock river incision that is amplified by the presence of waterfalls and knickzones. Whereas there is a robust monotonic relationship between channel steepness index and erosion rate for channels at steady state in the San Gabriel Mountains (DiBiase et al., 2010; DiBiase and Whipple, 2011), knickzones associated with channel adjustment to base-level fall show a wide range of behavior. Notably, these differences are difficult to resolve from analysis of individual long profiles. In this section, we highlight the key factors that preclude using a single, stream-power–type erosion law for analyzing both steady and transient channel incision, and we discuss the implications of waterfalls and knickzones for interpreting transient landscapes.

First, because process transitions associated with waterfalls and knickzones may both accelerate and slow landscape response times, caution is required when interpreting uplift history using modern channel long profiles (e.g., Roberts and White, 2010; Goren et al., 2014). For example, based on a calibrated stream-power–type relationship between channel steepness index and erosion rate for steady-state channels in the San Gabriel Mountains, the knickzone on Chilao Creek is predicted to erode at >1 mm/yr, which would imply waterfall migration rates more than an order of magnitude higher than observed. Moreover, applying a single set of parameters (m and n in Eq. 1) precludes accounting for both slow and fast knickzone behavior. At the least, quantification of spatial variations in bed cover, channel geometry, and grain size is needed to interpret relative incision rates. Even with such measurements, quantitative interpretation of river long profiles requires independent constraints on erosion rate (e.g., Kirby and Whipple, 2012; Mackey et al., 2014).

Second, observations of rapidly retreating waterfalls are at odds with predictions from bed-load saltation-abrasion incision models, which predict decreasing erosion rates at high transport stages due to increasing particle hop lengths (Sklar and Dietrich, 2004; Wobus et al., 2006a; Crosby et al., 2007). Two factors likely account for this discrepancy: Inclusion of erosion by suspended load abrasion is expected to be important at high transport stages (Lamb et al., 2008a; Scheingross et al., 2014), and a switch in process to waterfall retreat via plunge-pool drilling likely occurs (Howard et al., 1994; Lamb et al., 2007). Incorporating such processes is thus critical for predicting short-term landscape response times to changing boundary conditions. In particular, if knickzone retreat is rapid, then the following considerations arise: Strath terraces will be time-transgressive and require careful sampling techniques (Reusser et al., 2004; Haviv et al., 2006); the reach downstream of the knickzone will be less steep than its final steady-state slope, which may lead to misleading interpretations of uplift and erosion; and erosion rate measurements from detrital cosmogenic nuclides may be strongly biased by undosed sediment derived from waterfall erosion processes (though this effect may be lessened in the case of waterfall retreat by plucking or toppling of large blocks; Mackey et al., 2014).

We emphasize that many of the proposed controls on waterfall retreat rate are similar to the controls on fluvial bedrock incision (Whipple et al., 2000; Sklar and Dietrich, 2004), and that the retreat patterns of both waterfalls and slope-break knickpoints tend to have similar power-law dependencies on drainage area. Furthermore, slope-break knickpoints are often colocated with waterfalls (Crosby and Whipple, 2006; Berlin and Anderson, 2007; Lamb et al., 2014; Mackey et al., 2014). Thus, it is unclear whether waterfall and knickzone retreat drives landscape adjustment, or if adjustment is driven by differential incision of relict and downstream reaches. In Big Tujunga Creek, we argue that the presence of waterfalls and large boulders in the knickzone of Chilao Creek preserves the relict landscape of Chilao Flats—either these waterfalls are responsible for stalling slope-break knickpoint retreat, or they are simply a reflection of slowed incision due to a combination of boulder cover and resistant lithology. For the middle knickpoint on Big Tujunga Creek, the role of waterfalls in driving long-term landscape evolution is less clear, and it remains plausible that waterfall retreat is limited by downstream vertical channel incision and sediment transport, as indicated by the similar slope-break knickpoint retreat rates for channels with differing degrees of knickzones and waterfalls. For the lower knickzone, channel adjustment occurs primarily by waterfall and knickzone retreat.

Understanding the degree to which channel adjustment is driven by fluvial incision or by knickzone or waterfall retreat also has implications for the way in which sediment is delivered to depositional basins. For example, in the stream-power framework, an increase in uplift rate results in a gradual increase in sediment yield at the outlet until a balance between uplift and erosion is achieved. In the case of slow waterfalls or knickzones, this signal will be protracted, but still gradual. If, instead, the transient adjustment of the channel network is driven by rapid waterfall or knickzone retreat, then sediment delivery will be pulsed, and also strongly dependent on the nature of transient hillslope relaxation in inner gorges (Mackey et al., 2014). Additionally, the sediment yield pulses driven by waterfall retreat may introduce oscillations into the fan-catchment system that help sustain the mechanism of waterfall generation via fault-slip burial and exhumation, described earlier herein.

Ideally, a model for bedrock incision should be able to explain both steady-state relationships between channel form and erosion rate, and the transient response to changing boundary conditions (Lague, 2014). Although hypothesized to influence river incision, spatial variations in sediment supply, grain size, and channel geometry do not appear to exert do not appear to exert a first order control on channel long-profile form or erosion rate in steady-state landscapes (DiBiase and Whipple, 2011). It might be hoped that such complexities are masked during transient adjustment as well, but our observations in Big Tujunga Creek indicate that a detailed accounting of sediment cover, channel geometry, and transition to waterfall processes is required to faithfully reproduce the behavior of channels responding to changing boundary conditions.

CONCLUSIONS

Two prominent slope-break knickpoints separate three physiographic zones within Big Tujunga Creek, recording a two-stage sustained increase in uplift rate along the range-bounding Sierra Madre fault zone. In contrast to predictions from widely used bedrock incision laws, these slope-break knickpoints are associated with locally oversteepened knickzone reaches often consisting of multiple waterfalls. Additionally, a third knickzone, headed by Lower Big Tujunga Falls, lies within the lowest physiographic zone and offsets channels of similar steepness. These three knickzones are associated with over 800 individual waterfalls on main-stem and tributary channels—an observation that is at odds with prior interpretations of Big Tujunga Creek as a type example of detachment-limited stream-power incision. We used a conceptual long-profile model to show how knickzones and waterfalls may influence slope-break knickpoint retreat, by being either slow or fast relative to predictions based on

linear stream-power models. We tested these predictions in Big Tujunga Creek using patterns of tributary long profiles, strath terraces, cosmogenic erosion rates, channel bed conditions, and hillslope morphology. The upper slope-break knickpoint, characterized by a 275-m-high knickzone consisting of 15 waterfalls and intervening boulder-mantled channel reaches, is slowly retreating or stalled, and it preserves the relict topography of Chilao Flats. This relict topography also provides a mechanism to further slow knickzone and waterfall retreat as upstream drainage area shrinks and the sediment load to channels is dominated by sandy grus and local boulder collapse rather than coarse mobile bed load. The expression of waterfalls and knickzones on the network retreat pattern of the middle knickpoints is not straightforward, and there is evidence for both slow and fast knickzone behavior. This variability does not appear to be tied to the presence or magnitude of steep and waterfall-rich downstream reaches. Instead, we hypothesize that slope-break knickpoint retreat and knickzone development are controlled by spatial variations in hillslope sediment supply and rock strength. Furthermore, we show that moderate deviations from assumptions of uniform channel steepness of the relict landscape can introduce significant scatter into the elevation distribution of slope-break knickpoints, even in the absence of knickzones and waterfalls. Last, Lower Big Tujunga Falls and its associated knickzone are rapidly retreating relative to background channel incision and leave behind a wake of young strath terraces and an inner gorge consisting of oversteepened hillslopes. Overall, our results indicate that knickzone and associated slope-break knickpoint propagation slows down with increasing distance upstream, beyond expectations based on simple drainage-area–dependent knickpoint celerity models. Near the range front, we hypothesize that fast knickzones are generated by dynamics among alluvial-fan deposition, uplift, and channel incision, resulting in an assortment of waterfalls, inner gorges, and strath terraces that overprint longer-term signals. Upstream waterfalls, where preserved, insulate relict topography from modern base level by slowing or stalling slope-break knickpoint retreat. Thus, waterfalls and knickzones can play a significant role in modulating landscape adjustment time scales—an effect that is not currently accounted for in landscape evolution models.

ACKNOWLEDGMENTS

We thank B. Adams, N. Gasparini, M. Jungers, and D. Stolar for intrepid field assistance, and J. Scheingross and L. Malatesta for valuable discussions and feedback. Comments from two anonymous reviewers and the associate editor helped improve the manuscript. Funding for this project was provided by the National Science Foundation Geomorphology and Land Use Dynamics program (EAR-0724194 to Whipple, EAR-0518998 to Heimsath, and EAR-1147381 to Lamb). Laser altimetry data were acquired and processed by the National Center for Airborne Laser Mapping (NCALM) with support from Arizona State University (Whipple and Heimsath), Caltech (Lamb), and the U.S. Geological Survey.

REFERENCES CITED

Anderson, R.S., Repka, J.L., and Dick, G.S., 1996, Explicit treatment of inheritance in dating depositional surfaces using in situ Be-10 and Al-26: Geology, v. 24, p. 47–51, doi:10.1130/0091-7613(1996)024<0047:etoiid>2.3.co;2.

Attal, M., Cowie, P.A., Whittaker, A.C., Hobley, D., Tucker, G.E., and Roberts, G.P., 2011, Testing fluvial erosion models using the transient response of bedrock rivers to tectonic forcing in the Apennines, Italy: Journal of Geophysical Research, v. 116, F02005, doi:10.1029/2010JF001875.

Balco, G., Stone, J.O., Lifton, N.A., and Dunai, T.J., 2008, A complete and easily accessible means of calculating surface exposure ages or erosion rates from (10)Be and (26)Al measurements: Quaternary Geochronology, v. 3, p. 174–195, doi:10.1016/j.quageo.2007.12.001.

Baldwin, J.A., Whipple, K.X., and Tucker, G.E., 2003, Implications of the shear stress river incision model for the timescale of postorogenic decay of topography: Journal of Geophysical Research–Solid Earth, v. 108, 2158, doi:10.1029/2001jb000550.

Berlin, M.M., and Anderson, R.S., 2007, Modeling of knickpoint retreat on the Roan Plateau, western Colorado: Journal of Geophysical Research, v. 112, F03S06, doi:10.1029/2006jf000553.

Berlin, M.M., and Anderson, R.S., 2009, Steepened channels upstream of knickpoints: Controls on relict landscape response: Journal of Geophysical Research, v. 114, F03018, doi:10.1029/2008jf001148.

Bierman, P., and Gillespie, A., 1991, Range fires—A significant factor in exposure-age determination and geomorphic surface evolution: Geology, v. 19, p. 641–644, doi:10.1130/0091-7613(1991)019<0641:rfasfi>2.3.co;2.

Bishop, P., Hoey, T.B., Jansen, J.D., and Artza, I.L., 2005, Knickpoint recession rate and catchment area: The case of uplifted rivers in eastern Scotland: Earth Surface Processes and Landforms, v. 30, p. 767–778, doi:10.1002/esp.1191.

Blisniuk, K., Rockwell, T., Owen, L.A., Oskin, M., Lippincott, C., Caffee, M.W., and Dortch, J., 2010, Late Quaternary slip rate gradient defined using high-resolution topography and (10)Be dating of offset landforms on the southern San Jacinto fault zone, California: Journal of Geophysical Research–Solid Earth, v. 115, B08401, doi:10.1029/2009jb006346.

Blum, M.D., and Tornqvist, T.E., 2000, Fluvial responses to climate and sea-level change: A review and look forward: Sedimentology, v. 47, p. 2–48, doi:10.1046/j.1365-3091.2000.00008.x.

Blythe, A.E., Burbank, D.W., Farley, K.A., and Fielding, E.J., 2000, Structural and topographic evolution of the central Transverse Ranges, California, from apatite fission-track, (U-Th)/He and digital elevation model analyses: Basin Research, v. 12, p. 97–114, doi:10.1046/j.1365-2117.2000.00116.x.

Blythe, A.E., House, M.A., and Spotila, J.A., 2002, Low-temperature thermochronology of the San Gabriel and San Bernardino Mountains, southern California: Constraining structural evolution, *in* Barth, A., ed., Contributions to Crustal Evolution of the Southwestern United States: Geological Society of America Special Paper 365, p. 231–250, doi:10.1130/0-8137-2365-5.231.

Bookhagen, B., and Strecker, M.R., 2012, Spatiotemporal trends in erosion rates across a pronounced rainfall gradient: Examples from the southern central Andes: Earth and Planetary Science Letters, v. 327, p. 97–110, doi:10.1016/j.epsl.2012.02.005.

Bull, W.B., 1991, Geomorphic Responses to Climatic Change: Oxford, UK, Oxford University Press, 326 p.

Cannon, S.H., and Gartner, J.E., 2005, Wildfire-related debris flow from a hazards perspective, *in* Jakob, M., and Hungr, O., eds., Debris-Flow Hazards and Related Phenomena: Berlin, Springer, p. 363–385.

Chatanantavet, P., and Parker, G., 2009, Physically based modeling of bedrock incision by abrasion, plucking, and macroabrasion: Journal of Geophysical Research–Earth Surface, v. 114, F04018, doi:10.1029/2008jf001044.

Clark, M.K., Maheo, G., Saleeby, J., and Farley, K.A., 2005, The non-equilibrium landscape of the southern Sierra Nevada, California: GSA Today, v. 15, no. 9, p. 4–10.

Clark, M.K., Royden, L.H., Whipple, K.X., Burchfiel, B.C., Zhang, X., and Tang, W., 2006, Use of a regional, relict landscape to measure vertical deformation of the eastern Tibetan Plateau: Journal of Geophysical Research, v. 111, F03002, doi:10.1029/2005jf000294.

Cook, K.L., Turowski, J.M., and Hovius, N., 2013, A demonstration of the importance of bedload transport for fluvial bedrock erosion and knickpoint propagation: Earth Surface Processes and Landforms, v. 38, p. 683–695, doi:10.1002/esp.3313.

Cooke, M.L., and Dair, L.C., 2011, Simulating the recent evolution of the southern big bend of the San Andreas fault, southern California: Journal of Geophysical Research–Solid Earth, v. 116, B04405, doi:10.1029/2010jb007835.

Crosby, B.T., and Whipple, K.X., 2006, Knickpoint initiation and distribution within fluvial networks: 236 waterfalls in the Waipaoa River, North Island, New Zealand: Geomorphology, v. 82, p. 16–38, doi:10.1016/j.geomorph.2005.08.023.

Crosby, B.T., Whipple, K.X., Gasparini, N.M., and Wobus, C.W., 2007, Formation of fluvial hanging valleys: Theory and simulation: Journal of Geophysical Research, v. 112, F03S10, doi:10.1029/2006JF000566.

DiBiase, R.A., and Whipple, K.X., 2011, The influence of erosion thresholds and runoff variability on the relationships among topography, climate, and erosion rate: Journal of Geophysical Research, v. 116, F04036, doi:10.1029/2011JF002095.

DiBiase, R.A., Whipple, K.X., Heimsath, A.M., and Ouimet, W.B., 2010, Landscape form and millennial erosion rates in the San Gabriel Mountains, CA: Earth and Planetary Science Letters, v. 289, p. 134–144, doi:10.1016/j.epsl.2009.10.036.

DiBiase, R.A., Heimsath, A.M., and Whipple, K.X., 2012, Hillslope response to tectonic forcing in threshold landscapes: Earth Surface Processes and Landforms, v. 37, p. 855–865, doi:10.1002/esp.3205.

Dixon, J.L., Hartshorn, A.S., Heimsath, A.M., DiBiase, R.A., and Whipple, K.X., 2012, Chemical weathering response to tectonic forcing: A soils perspective from the San Gabriel Mountains, California: Earth and Planetary Science Letters, v. 323–324, p. 40–49, doi:10.1016/j.epsl.2012.01.010.

Eckis, R., 1928, Alluvial fans of the Cucamonga District, Southern California: The Journal of Geology, v. 36, p. 224–247, doi:10.2307/30060525.

Egholm, D.L., Knudsen, M.F., and Sandiford, M., 2013, Lifespan of mountain ranges scaled by feedbacks between landsliding and erosion by rivers: Nature, v. 498, p. 475–478, doi:10.1038/nature12218.

Finnegan, N.J., 2013, Interpretation and downstream correlation of bedrock river terrace treads created from propagating knickpoints: Journal of Geophysical Research–Earth Surface, v. 118, p. 54–64, doi:10.1029/2012jf002534.

Finnegan, N.J., and Balco, G., 2013, Sediment supply, base level, braiding, and bedrock river terrace formation: Arroyo Seco, California, USA: Geological Society of America Bulletin, v. 125, p. 1114–1124, doi:10.1130/b30727.1.

Finnegan, N.J., and Dietrich, W.E., 2011, Episodic bedrock strath terrace formation due to meander migration and cutoff: Geology, v. 39, p. 143–146, doi:10.1130/g31716.1.

Finnegan, N.J., Sklar, L.S., and Fuller, T.K., 2007, Interplay of sediment supply, river incision, and channel morphology revealed by the transient evolution of an experimental bedrock channel: Journal of Geophysical

Research–Earth Surface, v. 112, F03S11, doi:10.1029/2006jf000569.

Flint, J., 1974, Stream gradient as a function of order, magnitude, and discharge: Water Resources Research, v. 10, p. 969–973, doi:10.1029/WR010i005p00969.

Frankel, K.L., Pazzaglia, F.J., and Vaughn, J.D., 2007, Knickpoint evolution in a vertically bedded substrate, upstream-dipping terraces, and Atlantic slope bedrock channels: Geological Society of America Bulletin, v. 119, p. 476–486, doi:10.1130/b25965.1.

Gallen, S.F., Wegmann, K.W., Frankel, K.L., Hughes, S., Lewis, R.Q., Lyons, N., Paris, P., Ross, K., Bauer, J.B., and Witt, A.C., 2011, Hillslope response to knickpoint migration in the Southern Appalachians: Implications for the evolution of post-orogenic landscapes: Earth Surface Processes and Landforms, v. 36, p. 1254–1267, doi:10.1002/esp.2150.

Gardner, T.W., 1983, Experimental study of knickpoint and longitudinal profile evolution in cohesive, homogeneous material: Geological Society of America Bulletin, v. 94, p. 664–672, doi:10.1130/0016-7606(1983)94<664:esokal>2.0.co;2.

Gasparini, N.M., Whipple, K.X., and Bras, R.L., 2007, Predictions of steady state and transient landscape morphology using sediment-flux–dependent river incision models: Journal of Geophysical Research, v. 112, F03S09, doi:10.1029/2006JF000567.

Gilbert, G.K., 1907, Rate of Recession of Niagara Falls: U.S. Geological Survey Bulletin 306, p. 1–31.

Goren, L., Fox, M., and Willett, S.D., 2014, Tectonics from fluvial topography using formal linear inversion: Theory and applications to the Inyo Mountains, California: Journal of Geophysical Research–Earth Surface (in press), doi:10.1002/2014JF003079.

Hancock, G.S., Anderson, R.S., and Whipple, K.X., 1998, Beyond power: Bedrock river incision process and form, *in* Tinkler, K.J., and Wohl, E.E., eds., Rivers Over Rock: Fluvial Processes in Bedrock Channels: American Geophysical Union Geophysical Monograph 107, p. 35–60, doi:10.1029/GM107p0035.

Hartshorn, K., Hovius, N., Dade, W.B., and Slingerland, R.L., 2002, Climate-driven bedrock incision in an active mountain belt: Science, v. 297, p. 2036–2038, doi:10.1126/science.1075078.

Haviv, I., Enzel, Y., Whipple, K.X., Zilberman, E., Stone, J., Matmon, A., and Fifield, L.K., 2006, Amplified erosion above waterfalls and oversteepened bedrock reaches: Journal of Geophysical Research–Earth Surface, v. 111, F04004, doi:10.1029/2006jf000461.

Haviv, I., Enzel, Y., Whipple, K.X., Zilberman, E., Matmon, A., Stone, J., and Fifield, K.L., 2010, Evolution of vertical knickpoints (waterfalls) with resistant caprock: Insights from numerical modeling: Journal of Geophysical Research, v. 115, F03028, doi:10.1029/2008jf001187.

Hayakawa, Y., and Matsukura, Y., 2003, Recession rates of waterfalls in Boso Peninsula, Japan, and a predictive equation: Earth Surface Processes and Landforms, v. 28, p. 675–684, doi:10.1002/esp.519.

Hayakawa, Y.S., and Oguchi, T., 2006, DEM-based identification of fluvial knickzones and its application to Japanese mountain rivers: Geomorphology, v. 78, p. 90–106, doi:10.1016/j.geomorph.2006.01.018.

Heimsath, A.M., DiBiase, R.A., and Whipple, K.X., 2012, Soil production limits and the transition to bedrock dominated landscapes: Nature Geoscience, v. 5, p. 210–214, doi:10.1038/ngeo1380.

Hilley, G.E., and Arrowsmith, J.R., 2008, Geomorphic response to uplift along the Dragon's Back pressure ridge, Carrizo Plain, California: Geology, v. 36, p. 367–370, doi:10.1130/G24517A.1.

Howard, A.D., Dietrich, W.E., and Seidl, M.A., 1994, Modeling fluvial erosion on regional to continental scales: Journal of Geophysical Research–Solid Earth, v. 99, p. 13,971–13,986, doi:10.1029/94jb00744.

Jansen, J.D., Fabel, D., Bishop, P., Xu, S., Schnabel, C., and Codilean, A.T., 2011, Does decreasing paraglacial sediment supply slow knickpoint retreat?: Geology, v. 39, p. 543–546, doi:10.1130/g32018.1.

Johnson, J.P., and Whipple, K.X., 2007, Feedbacks between erosion and sediment transport in experimental bedrock channels: Earth Surface Processes and Landforms, v. 32, p. 1048–1062, doi:10.1002/esp.1471.

Kirby, E., and Whipple, K.X., 2012, Expression of active tectonics in erosional landscapes: Journal of Structural Geology, v. 44, p. 54–75, doi:10.1016/j.jsg.2012.07.009.

Kirby, S.M., Janecke, S.U., Dorsey, R.J., Housen, B.A., Langenheim, V.E., McDougall, K.A., and Steely, A.N., 2007, Pleistocene Brawley and Ocotillo Formations: Evidence for initial strike-slip deformation along the San Felipe and San Jacinto fault zones, southern California: The Journal of Geology, v. 115, p. 42–62, doi:10.1086/509248.

Kohl, C.P., and Nishiizumi, K., 1992, Chemical isolation of quartz for measurement of in-situ–produced cosmogenic nuclides: Geochimica et Cosmochimica Acta, v. 56, p. 3583–3587, doi:10.1016/0016-7037(92)90401-4.

Lague, D., 2014, The stream power river incision model: Evidence, theory and beyond: Earth Surface Processes and Landforms, v. 39, p. 38–61, doi:10.1002/esp.3462.

Lague, D., Hovius, N., and Davy, P., 2005, Discharge, discharge variability, and the bedrock channel profile: Journal of Geophysical Research, v. 110, F04006, doi:10.1029/2004JF000259.

Lal, D., 1991, Cosmic ray labeling of erosion surfaces: In situ nuclide production rates and erosion models: Earth and Planetary Science Letters, v. 104, p.424–439, doi:10.1016/0012-821X(91)90220-C.

Lamb, M.P., and Dietrich, W.E., 2009, The persistence of waterfalls in fractured rock: Geological Society of America Bulletin, v. 121, p. 1123–1134, doi:10.1130/b26482.1.

Lamb, M.P., Howard, A.D., Dietrich, W.E., and Perron, J.T., 2007, Formation of amphitheater-headed valleys by waterfall erosion after large-scale slumping on Hawai'i: Geological Society of America Bulletin, v. 119, p. 805–822, doi:10.1130/B25986.1.

Lamb, M.P., Dietrich, W.E., and Sklar, L.S., 2008a, A model for fluvial bedrock incision by impacting suspended and bed load sediment: Journal of Geophysical Research, v. 113, F03025, doi:10.1029/2007JF000915.

Lamb, M.P., Dietrich, W.E., and Venditti, J.G., 2008b, Is the critical Shields stress for incipient sediment motion dependent on channel-bed slope?: Journal of Geophysical Research–Earth Surface, v. 113, F02008, doi:10.1029/2007jf000831.

Lamb, M.P., Scheingross, J.S., Amidon, W.H., Swanson, E., and Limaye, A., 2011, A model for fire-induced sediment yield by dry ravel in steep landscapes: Journal of Geophysical Research–Earth Surface, v. 116, F03006, doi:10.1029/2010JF001878.

Lamb, M.P., Mackey, B.H., and Farley, K.A., 2014, Amphitheater-headed canyons formed by megaflooding at Malad Gorge, Idaho: Proceedings of the National Academy of Sciences of the United States of America, v. 111, p. 57–62, doi:10.1073/pnas.1312251111.

Lavé, J., and Burbank, D.W., 2004, Denudation processes and rates in the Transverse Ranges, southern California: Erosional response of a transitional landscape to external and anthropogenic forcing: Journal of Geophysical Research, v. 109, F01006, doi:10.1029/2003JF000023.

Lindvall, S.C., and Rubin, C.M., 2008, Slip Rate Studies along the Sierra Madre–Cucamonga Fault System Using Geomorphic and Cosmogenic Surface Exposure Age Constraints: Collaborative Research with Central Washington University and William Lettis & Associates, Inc.: U.S. Geological Survey Final Report 03HQGR0084, 13 p.

Lutz, A.T., Dorsey, R.J., Housen, B.A., and Janecke, S.U., 2006, Stratigraphic record of Pleistocene faulting and basin evolution in the Borrego Badlands, San Jacinto fault zone, Southern California: Geological Society of America Bulletin, v. 118, p. 1377–1397, doi:10.1130/B25946.1.

Mackey, B.H., Scheingross, J.S., Lamb, M.P., and Farley, K.A., 2014, Knickpoint formation, rapid propagation, and landscape response following coastal cliff retreat at the last interglacial sea-level highstand: Kaua'i, Hawai'i: Geological Society of America Bulletin (in press), doi:10.1130/B30930.1.

Marshall, S.T., Cooke, M.L., and Owen, S.E., 2009, Interseismic deformation associated with three-dimensional faults in the greater Los Angeles region, California: Journal of Geophysical Research–Solid Earth, v. 114, B12403, doi:10.1029/2009jb006439.

Matti, J.C., and Morton, D.M., 1993, Paleogeographic evolution of the San Andreas fault in southern California: A reconstruction based on a new cross-fault correlation, *in* Powell, R.E., Weldon, R.J., II, and Matti, J.C., eds., The San Andreas Fault System: Displacement, Palinspastic Reconstruction, and Geologic Evolution: Geological Society of America Memoir 178, p. 107–159, doi:10.1130/MEM178-p107.

Meade, B.J., and Hager, B.H., 2005, Block models of crustal motion in southern California constrained by GPS measurements: Journal of Geophysical Research–Solid Earth, v. 110, B03403, doi:10.1029/2004jb003209.

Miller, S.R., Baldwin, S.L., and Fitzgerald, P.G., 2012, Transient fluvial incision and active surface uplift in the Woodlark Rift of eastern Papua New Guinea: Lithosphere, v. 4, p. 131–149, doi:10.1130/l135.1.

Morton, D.M., and Matti, J.C., 1993, Extension and contraction within an evolving divergent strike-slip fault complex: The San Andreas and San Jacinto fault zones at their convergence in southern California, *in* Powell, R.E., Weldon, R.J., II, and Matti, J.C., eds., The San Andreas Fault System: Displacement, Palinspastic Reconstruction, and Geologic Evolution: Geological Society of America Memoir 178, p. 217–230, doi:10.1130/MEM178-p217.

Mueller, M., 2013, Assessing the Role of the San Andreas Fault in Controlling the Spatial Distribution of Erosion Rates in the Transverse Ranges, Southern California [M.S. thesis]: Ann Arbor, Michigan, University of Michigan, 53 p.

Niemann, J.D., Gasparini, N.M., Tucker, G.E., and Bras, R.L., 2001, A quantitative evaluation of Playfair's law and its use in testing long-term stream erosion models: Earth Surface Processes and Landforms, v. 26, p. 1317–1332, doi:10.1002/esp.272.

Ortega, J.A., Wohl, E., and Livers, B., 2013, Waterfalls on the eastern side of Rocky Mountain National Park, Colorado, USA: Geomorphology, v. 198, p. 37–44, doi:10.1016/j.geomorph.2013.05.010.

Ouimet, W.B., Whipple, K.X., Royden, L.H., Sun, Z.M., and Chen, Z.L., 2007, The influence of large landslides on river incision in a transient landscape: Eastern margin of the Tibetan Plateau (Sichuan, China): Geological Society of America Bulletin, v. 119, p. 1462–1476, doi:10.1130/B26136.1.

Ouimet, W.B., Whipple, K.X., and Granger, D.E., 2009, Beyond threshold hillslopes: Channel adjustment to base-level fall in tectonically active mountain ranges: Geology, v. 37, p. 579–582, doi:10.1130/G30013A.1.

Paola, C., Heller, P.L., and Angevine, C.L., 1992, The large-scale dynamics of grain-size variation in alluvial basins: 1. Theory: Basin Research, v. 4, p. 73–90, doi:10.1111/j.1365-2117.1992.tb00145.x.

Parker, G., Wilcock, P.R., Paola, C., Dietrich, W.E., and Pitlick, J., 2007, Physical basis for quasi-universal relations describing bankfull hydraulic geometry of single-thread gravel bed rivers: Journal of Geophysical Research–Earth Surface, v. 112, F04005, doi:10.1029/2006jf000549.

Perron, J.T., and Royden, L., 2013, An integral approach to bedrock river profile analysis: Earth Surface Processes and Landforms, v. 38, p. 570–576, doi:10.1002/esp.3302.

Peterson, M.D., and Wesnousky, S.G., 1994, Fault slip rates and earthquake histories for active faults in Southern California: Bulletin of the Seismological Society of America, v. 84, p. 1608–1649.

Reinhardt, L.J., Hoey, T.B., Barrows, T.T., Dempster, T.J., Bishop, P., and Fifield, L.K., 2007, Interpreting erosion rates from cosmogenic radionuclide concentrations measured in rapidly eroding terrain: Earth Surface Processes and Landforms, v. 32, p. 390–406, doi:10.1002/esp.1415.

Reusser, L.J., Bierman, P.R., Pavich, M.J., Zen, E.A., Larsen, J., and Finkel, R., 2004, Rapid late Pleistocene incision of Atlantic passive-margin river gorges: Science, v. 305, p. 499–502, doi:10.1126/science.1097780.

Roberts, G.G., and White, N., 2010, Estimating uplift rate histories from river profiles using African examples:

Journal of Geophysical Research–Solid Earth, v. 115, B02406, doi:10.1029/2009jb006692.

Royden, L., and Perron, J.T., 2013, Solutions of the stream power equation and application to the evolution of river longitudinal profiles: Journal of Geophysical Research–Earth Surface, v. 118, p. 497–518, doi:10.1002/jgrf.20031.

Scheingross, J.S., Brun, F., Lo, D.Y., Omerdin, K., and Lamb, M.P., 2014, Experimental evidence for fluvial bedrock incision by suspended and bedload sediment: Geology, v. 42, p. 523–526, doi:10.1130/g35432.1.

Schoenbohm, L.M., Whipple, K.X., Burchfiel, B.C., and Chen, L., 2004, Geomorphic constraints on surface uplift, exhumation, and plateau growth in the Red River region, Yunnan Province, China: Geological Society of America Bulletin, v. 116, p. 895–909, doi:10.1130/B25364.1.

Scott, K.M., 1973, Scour and Fill in Tujunga Wash—A Fanhead Valley in Urban Southern California–1969: U.S. Geological Survey Professional Paper 732-B, 28 p.

Seidl, M., and Dietrich, W., 1992, The problem of channel erosion into bedrock: Catena, v. 23, supplement, p. 101–124.

Seidl, M.A., Dietrich, W.E., and Kirchner, J.W., 1994, Longitudinal profile development into bedrock: An analysis of Hawaiian channels: The Journal of Geology, v. 102, p. 457–474.

Seidl, M.A., Finkel, R.C., Caffee, M.W., Hudson, G.B., and Dietrich, W.E., 1997, Cosmogenic isotope analyses applied to river longitudinal profile evolution: Problems and interpretations: Earth Surface Processes and Landforms, v. 22, p. 195–209, doi:10.1002/(sici)1096-9837(199703)22:3<195:aid-esp748>3.0.co;2-0.

Sklar, L.S., and Dietrich, W.E., 2004, A mechanistic model for river incision into bedrock by saltating bed load: Water Resources Research, v. 40, W06301, doi:10.1029/2003WR002496.

Spotila, J.A., House, M.A., Blythe, A.E., Niemi, N.A., and Bank, G.C., 2002, Controls on the erosion and geomorphic evolution of the San Bernardino and San Gabriel Mountains, southern California, *in* Barth, A., ed., Contributions to Crustal Evolution of the Southwestern United States: Geological Society of America Special Paper 365, p. 205–230, doi:10.1130/0-8137-2365-5.205.

Stone, J.O., 2000, Air pressure and cosmogenic isotope production: Journal of Geophysical Research–Solid Earth v. 105, p. 23,753–23,759, doi:10.1029/2000JB900181.

Tucker, A.Z., and Dolan, J.F., 2001, Paleoseismologic evidence for a >8 ka age of the most recent surface rupture on the eastern Sierra Madre fault, northern Los Angeles Metropolitan Region, California: Bulletin of the Seismological Society of America, v. 91, p. 232–249, doi:10.1785/0120000093.

Tucker, G.E., 2004, Drainage basin sensitivity to tectonic and climatic forcing: Implications of a stochastic model for the role of entrainment and erosion thresholds: Earth Surface Processes and Landforms, v. 29, p. 185–205, doi:10.1002/esp.1020.

Valla, P.G., van der Beek, P.A., and Lague, D., 2010, Fluvial incision into bedrock: Insights from morphometric analysis and numerical modeling of gorges incising glacial hanging valleys (western Alps, France): Journal of Geophysical Research, v. 115, F02010, doi:10.1029/2008jf001079.

Weissel, J.K., and Seidl, M.A., 1997, Influence of rock strength properties on escarpment retreat across passive continental margins: Geology, v. 25, p. 631–634, doi:10.1130/0091-7613(1997)025<0631:iorspo>2.3.co;2.

Whipple, K.X., and Tucker, G.E., 1999, Dynamics of the stream-power river incision model: Implications for height limits of mountain ranges, landscape response timescales, and research needs: Journal of Geophysical Research–Solid Earth, v. 104, p. 17,661–17,674, doi:10.1029/1999JB900120.

Whipple, K.X., and Tucker, G.E., 2002, Implications of sediment-flux–dependent river incision models for landscape evolution: Journal of Geophysical Research–Solid Earth, v. 107, p. ETG 3-1–ETG 3-20, doi:10.1029/2000JB000044.

Whipple, K.X., Hancock, G.S., and Anderson, R.S., 2000, River incision into bedrock: Mechanics and relative efficacy of plucking, abrasion, and cavitation: Geological Society of America Bulletin, v. 112, p. 490–503, doi:10.1130/0016-7606(2000)112<490:RIIBMA>2.0.CO;2.

Whipple, K.X., DiBiase, R.A., and Crosby, B.T., 2013, Bedrock rivers, *in* Shroder, J.J., and Wohl, E., eds., Treatise on Fluvial Geomorphology, Volume 9: San Diego, California, Academic Press, p. 550–573.

Whittaker, A.C., and Boulton, S.J., 2012, Tectonic and climatic controls on knickpoint retreat rates and landscape response times: Journal of Geophysical Research–Earth Surface, v. 117, F02024, doi:10.1029/2011jf002157.

Whittaker, A.C., Attal, M., Cowie, P.A., Tucker, G.E., and Roberts, G., 2008, Decoding temporal and spatial patterns of fault uplift using transient river long profiles: Geomorphology, v. 100, p. 506–526, doi:10.1016/j.geomorph.2008.01.018.

Willett, S.D., McCoy, S.W., Perron, J.T., Goren, L., and Chen, C.-Y., 2014, Dynamic reorganization of river basins: Science, v. 343, no. 6175, doi:10.1126/science.1248765.

Wobus, C.W., Crosby, B.T., and Whipple, K.X., 2006a, Hanging valleys in fluvial systems: Controls on occurrence and implications for landscape evolution: Journal of Geophysical Research, v. 111, F02017, doi:10.1029/2005JF000406.

Wobus, C.W., Whipple, K.X., Kirby, E., Snyder, N.P., Johnson, J.P.L., Spyropolou, K., Crosby, B.T., and Sheehan, D., 2006b, Tectonics from topography: Procedures, promise, and pitfalls, *in* Willett, S.D., Hovius, N., Brandon, M.T., and Fisher, D.M., eds., Tectonics, Climate, and Landscape Evolution: Geological Society of America Special Paper 398, p. 55–74, doi:10.1130/2006.2398(04).

Wobus, C.W., Tucker, G.E., and Anderson, R.S., 2010, Does climate change create distinctive patterns of landscape incision?: Journal of Geophysical Research–Earth Surface, v. 115, F04008, doi:10.1029/2009jf001562.

Yanites, B.J., Ehlers, T.A., Becker, J.K., Schnellmann, M., and Heuberger, S., 2013, High magnitude and rapid incision from river capture: Rhine River, Switzerland: Journal of Geophysical Research–Earth Surface, v. 118, p. 1060–1084, doi:10.1002/jgrf.20056.

Science Editor: A. Hope Jahren
Associate Editor: Anne Jefferson

Manuscript Received 9 April 2014
Revised Manuscript Received 30 July 2014
Manuscript Accepted 5 September 2014

Printed in the USA